Pharmacological Research 194 (2023) 106847

Contents lists available at ScienceDirect

Pharmacological Research

journal homepage: www.elsevier.com/locate/yphrs

Invited review

Small molecule protein kinase inhibitors approved by regulatory agencies outside of the United States

Robert Roskoski Jr.

Blue Ridge Institute for Medical Research, 221 Haywood Knolls Drive, Hendersonville, NC 28791-8717, United States

ARTICLE INFO

Keywords:
Breast cancer
Chronic myelogenous leukemia
Lipinski rule of five
Lipophilic efficiency
Non-small cell lung cancer
Orally bioavailable

Chemical compounds studied in this article:
Apatinib (PubMED CID: 11315474)
Catequentinib (PubMED CID: 25017411)
Delgocitinib (PubMED CID: 50914062)
Fasudil (PubMED CID: 3547)
Filgotinib (PubMED CID: 49831257)
Icotinib (PubMED CID: 22024915)
Imatinib (PubMED CID: 123596)
Peficitinib (PubMED CID: 57928403)
Pyrotinib (PubMED CID: 51039030)
Tirabrutinib (PubMED CID: 54755438)

ABSTRACT

Owing to genetic alterations and overexpression, the dysregulation of protein kinases plays a significant role in the pathogenesis of many autoimmune and neoplastic disorders and protein kinase antagonists have become an important drug target. Although the efficacy of imatinib in the treatment of chronic myelogenous leukemia in the United States in 2001 was the main driver of protein kinase inhibitor drug discovery, this was preceded by the approval of fasudil (a ROCK antagonist) in Japan in 1995 for the treatment of cerebral vasospasm. There are 21 small molecule protein kinase inhibitors that are approved in China, Japan, Europe, and South Korea that are not approved in the United Sates and 75 FDA-approved inhibitors in the United States. Of the 21 agents, eleven target receptor protein-tyrosine kinases, eight inhibit nonreceptor protein-tyrosine kinases, and two block protein-serine/threonine kinases. All 21 drugs are orally bioavailable or topically effective. Of the non-FDA approved drugs, sixteen are prescribed for the treatment of neoplastic diseases, three are directed toward inflammatory disorders, one is used for glaucoma, and fasudil is used in the management of vasospasm. The leading targets of kinase inhibitors approved by both international regulatory agencies and by the FDA are members of the EGFR family, the VEGFR family, and the JAK family. One-third of the 21 internationally approved drugs are not compliant with Lipinski's rule of five for orally bioavailable drugs. The rule of five relies on four parameters including molecular weight, number of hydrogen bond donors and acceptors, and the Log of the partition coefficient.

1. The importance of therapeutic protein kinase inhibitors

Owing to genetic alterations and overexpression, the dysregulation of protein kinases plays a significant role in the pathogenesis of autoimmune, cardiovascular, inflammatory, and nervous diseases as well as many neoplastic disorders. Consequently, protein kinases are among the most important drug targets of the 21st century [1–4]. About 25–33% of drug discovery protocols worldwide are directed against these enzymes. The therapeutic efficacy of imatinib in the management of Philadelphia chromosome-positive chronic myelogenous leukemia in 2001 stimulated the search for orally effective protein kinase antagonists [5–7]. This unparalleled success resulted from the imatinib inhibition of the active chimeric BCR-Abl protein-tyrosine kinase, the causative biochemical defect that produces these leukemias. This was preceded by the approval of fasudil in Japan in 1995 for the treatment of vasospasm in people with subarachnoid hemorrhage [8]. This agent was discovered by investigators seeking calcium antagonists for vasospasm treatment [9,10]. However, experiments demonstrated that fasudil (HA1077) functions as a ROCK antagonist thus becoming the first small molecule protein kinase inhibitor approved by a regulatory agency. This

Abbreviations: ADMET, absorption, distribution, metabolism, excretion, and toxicity; ALL, acute lymphocytic leukemia; AML, acute myelogenous leukemia; bRo5, beyond Lipinski's rule of five; BTK, bruton protein-tyrosine kinase; CLL, chronic lymphocytic lymphoma; CML, chronic myelogenous leukemia; CRC, colorectal cancer; FDA, Food and Drug Administration of the United States; EGFR, epidermal growth factor receptor; FGFR, fibroblast growth factor receptor; Fsp^3, fraction of sp^3 carbon atoms/total carbon atoms; HA, hydrogen-bond acceptor; HD, hydrogen-bond donor; HTS, high throughput screening; JAK, Janus kinase; LE, ligand efficiency; LipE, lipophilic efficiency; MW, molecular weight; N, number of heavy (non-hydrogen) atoms; nAr, number of aromatic rings; nBnz, number of benzenes; nRng, number of rings; nRotB, number of rotatable bonds; NSCLC, non-small cell lung cancer; PDGFR, platelet-derived growth factor receptor; Ph^+, Philadelphia chromosome-positive; PI3-kinase, phosphatidylinositol 3-kinase; PSA, polar surface area; QED, quantitative estimate of drug-likeness; Ro5, Lipinski's rule of five; ROCK, Rho-associated coiled-coiled-containing kinase; SLL, small lymphocytic lymphoma; TCIs, Targeted Covalent Inhibitors; VEGFR, vascular endothelial growth factor receptor.

E-mail address: rrj@brimr.org.

https://doi.org/10.1016/j.phrs.2023.106847
Received 3 July 2023; Accepted 3 July 2023
Available online 15 July 2023

Table 1
Small molecule protein kinase inhibitors approved outside of the United States, their protein kinase targets, and therapeutic indications[a].

Drug	Code	Company	Trade name	Year approved & country[b]	Primary targets[c]	Therapeutic indications[d]
Fasudil	HA-1077	Chuanwai	Eril	1995 Japan, 2010 China	ROCK1/2	Cerebral vasospasm
Icotinib	BPI-2009 H	Zhejiang Betta Pharm	Conmana	2012 China	EGFR	NSCLC
Ripasudil	K-115	Kowa	Glanatec	2014 Japan	ROCK1/2	Glaucoma
Apatinib or rivoceranib	YN 968D1	Hengrui Pharm.	Aitan	2014 China	VEGFRs, Kit, Src	NSCLC and gastric cancer
Radotinib	IY5511	Daewoong Pharm	Supect	2015 KOR	BCR-Abl, PDGFR	Ph^+ CML
Olmutinib	BI 1482694	Boehringer Ingelheim	Olita	2016 KOR	EGFR T790M	NSCLC
Simotinib	SIM 6802	Jiangsu Simcere Pharm	Ximotini	2018 China	EGFR	NSCLC
Catequentinib or anlotinib	AL3818	Advenchen Lab	FOCUSV	2018 China	VEGFRs	NSCLC
Fruquintinib	HMPL-013	Chinai-Med Eli Lilly	Elunate	2018 China	VEGFRs	CRC
Flumatinib	HHGV678	Jiangsu Hansoh Pharm	Xinfu	2019 China	BCR-Abl, PDGFR	CML
Filgotinib	GS 0634	Galapagos NV	Jyseleca	2020 EMA, Japan	JAKs	Rheumatoid arthritis
Almonertinib or aumolertinib	HS 10296	Hansoh Pharm	Ameile	2020 China	EGFR T790M	NSCLC
Tirabrutinib	GS 4059	Ono Gilead	Velexbru	2020 Japan	BTK	CML
Delgocitinib	GTE 052	Japan Tobacco	Corectim	2020 Japan	JAKs	Atopic dermatitis
Pyrotinib	SHR 1258	Jiangsu Hengrui	Irene	2020 China	EGFR, HER2/4	Breast cancer
Orelabrutinib	ICP 022	InnoCare	Hybruka	2020 China	BTK	Mantle cell lymphoma, CLL, SLL
Peficitinib	ASP015K	Astellas Janssen	Smyraf	2021 Japan	JAKs	Rheumatoid arthritis
Surufatinib or sulfatinib	HMPL 012	Hutchmed	Sulanda	2021 China	VEGFRs	Pancreatic neuroendocrine tumor
Savolitinib	C104732	AZ Hutchmed	Orpathys	2021 China	MET	NSCLC
Lazertinib	YH25448	Yuhan-Janssen	Leclaza	2021 KOR	EGFR	NSCLC
Furmonertinib or alflutinib	AST 2018	Allist Pharm	Ivesa	2021 China	EGFR T790M	NSCLC

[a] Data from [12] and https://www.ppu.mrc.ac.uk/list-clinically-approved-kinase-inhibitors.
[b] EMA, European Medicines Agency; KOR, South Korea.
[c] Although many of these drugs are multikinase inhibitors, only the primary therapeutic targets are given here.
[d] CLL, chronic lymphocytic lymphoma; CML, chronic myelogenous leukemias; CRC, colorectal cancer; HER2/4, human epidermal growth factor receptor-2/4; NSCLC, non-small cell lung cancers; Ph^+, Philadelphia chromosome positive; SLL, small lymphocytic lymphoma.

medicinal was also approved in China in 2010 for the treatment of vasospasm, but it is not approved in the United States.

Approximately 250 orally effective protein kinase inhibitors are in clinical trials worldwide [11]. A complete catalogue of these drugs, which is regularly updated, can be found at www.icoa.fr/pkidb/. There are 75 FDA-approved medicines that inhibit about two dozen different protein kinases (www.brimr.org/PKI/PKIs.htm). However, these targets represent a small fraction of the 518-member protein kinase superfamily. Another 21 small molecule protein kinase inhibitors are approved in China, Japan, Europe, and South Korea (Table 1).

Manning et al. reported that the human protein kinase enzyme family contains 478 typical and 40 atypical members [13] including phosphatidylinositol 3-kinase (PI 3-kinase) [7,14]. Protein kinases catalyze the following reaction;.

$$MgATP^{1-} + protein\text{–}O{:}H \rightarrow protein\text{–}O{:}PO_3^{2-} + MgADP + H^+$$

Note that the phosphoryl group (PO_3^{2-}) and not the phosphate group (OPO_3^{2-}) is transferred during this reaction. Based upon the nature of the protein–O:H groups, these enzymes are classified as protein-serine/threonine kinases (385 members), protein-tyrosine kinases (90), and protein-tyrosine kinase–like enzymes (43). The protein-tyrosine kinase family consists of both transmembrane receptor (58) and intracellular nonreceptor (32) proteins. Moreover, the protein kinase family includes a small group of intracellular enzymes such as MEK1/2 that mediate the phosphorylation of both tyrosine and then threonine residues within the activation segment of their protein kinase targets; owing to this distinctive property, MEK1/2 and its congeners are labeled as dual specificity (DS) protein kinases. Another indication of the importance of the protein kinase family is the reckoning that one in every 40 human genes (518 protein kinase genes out of the presumed 20,000 human protein-encoding genes) corresponds to a protein kinase. Protein kinases consequently constitute about 2.5% of the human genome. A further indication of the importance of protein kinases as drug targets is the report of Manning et al. that indicates that 244 protein kinases map to cancer amplicons and other disease loci [13]. Consequently, as additional research on the pathogenesis of other diseases is performed, it is likely that there will be a significant increase in the number of protein kinase targets.

Regulatory agencies in China, Japan, Europe, and South Korea approved 21 small molecule therapeutic protein kinase inhibitors that are not approved in the United States [12] and these are the main focus of this article. Of these 21 drugs, eleven antagonize receptor protein-tyrosine kinases, eight inhibit nonreceptor protein-tyrosine kinases, and two block protein-serine/threonine kinases. Nearly all of these drugs are orally bioavailable. Of the 21 antagonists, ripasudil, which is approved for the treatment of glaucoma in Japan, is prescribed as an eyedrop and delgocitinib, which is approved for the treatment of atopic dermatitis in Japan, is a topical cream.

The FDA has approved 75 kinase inhibitors as of July 2023. Of these 75 drugs, forty block receptor protein-tyrosine kinases, nineteen target nonreceptor protein-tyrosine kinases, twelve are directed against protein-serine/threonine protein kinases, and four are directed against dual specificity protein kinases (MEK1/2) [3,4]. Nearly all of these are orally effective with the exceptions of temsirolimus and trilaciclib (which are given intravenously) and netarsudil (an eye drop). Ruxolitinib is an orally effective JAK1/2 protein kinase inhibitor that was approved for the treatment of myelofibrosis and polycythemia vera in 2011. This medicinal is topically active as a cream and was approved in 2021 for the treatment of atopic dermatitis [3].

Of the 21 non-FDA approved drugs considered in this article, sixteen are prescribed for the treatment of neoplastic disease (12 for solid tumors such as breast, colon, lung, and stomach cancers, three against nonsolid tumors such as leukemia, and one against both types of neoplasm: orelabrutinib) (Table 1). Of the FDA-approved medicines, the data indicate that 63 of these medicinals are approved for the management of neoplasms (51 against solid tumors, eight against nonsolid tumors, and four against both types of tumors) [3,4]. Oral medicines are the patient-preferred method of drug administration. When compared with intravenous therapy, the quality of life for patients is improved because of the ability to self-administer at home. Most drugs used in cancer therapy are given intravenously, but most people prefer the convenience of oral drugs. Pills have many advantages in comparison with other drug formulations. In contrast to liquids or suspensions, solid forms of oral drugs are more stable during storage [15].

Five of the drugs approved outside of the United States form covalent bonds with their enzyme targets and they are therefore classified as TCIs (targeted covalent inhibitors) [16]. These include olmutinib,

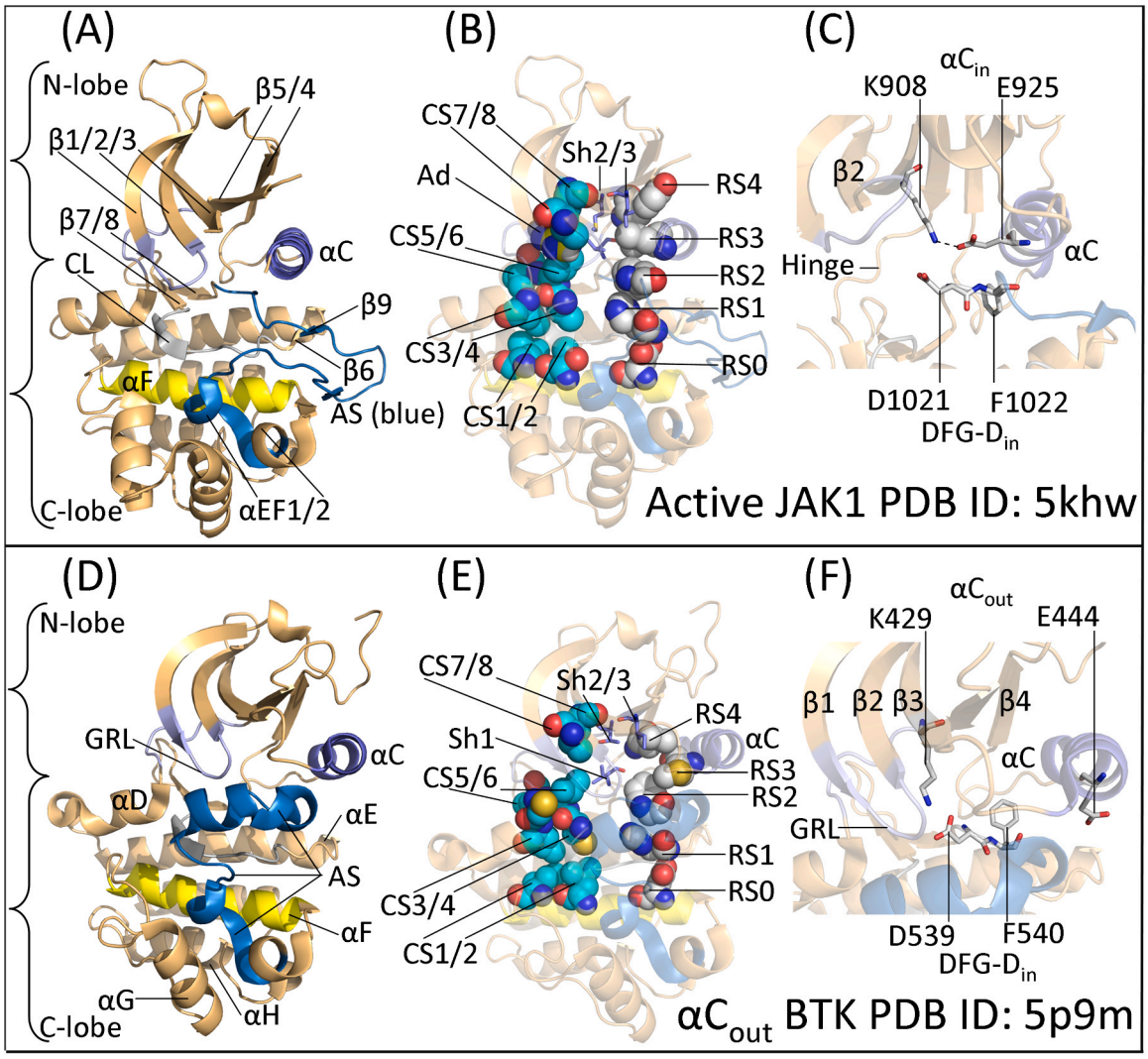

Fig. 1. (A) Overview of active JAK1 with an open activation segment and (B) its C-spine and R-spine residues. (C) The αC_{in} and DFG-D_{in} conformation of active JAK1 – dashes represent a salt bridge. (D) Overview of inactive BTK with a closed activation segment and (E) its C-spine and R-spine residues. (F) The αC_{out} and DFG-D_{in} structure of dormant BTK. Ad, adenine; CS, catalytic spine; GRL, glycine-rich loop; PDB ID, protein database identification number; RS regulatory spine. Figs. 1, 2, 5, and 6 were prepared using the PyMOL Molecular Graphics System Version 1.5.0.4 Schrödinger, LLC.

almonertinib, lazertinib, and furmonertinib (each inhibiting EGFR in NSCLC) and orelabrutinib (blocking BTK in mantle cell lymphoma, chronic lymphocytic leukemia (CLL), and small cell lymphoma (SLL)). Eight of the FDA-approved kinase inhibitors form covalent bonds with their target enzymes. These agents include acalabrutinib (antagonizing BTK in mantle cell lymphoma), afatinib (blocking EGFR in NSCLC), dacomitinib (inhibiting mutant EGFR in NSCLC), ibrutinib (targeting BTK in chronic lymphocytic leukemia, mantle cell lymphoma, marginal zone lymphoma, chronic graft vs. host disease, and Waldenström macroglobulinemia), neratinib (inhibiting ErbB2 in HER2-positive breast cancer), osimertinib (targeting *EGFR T970M* mutants in NSCLC), ritlecitinb (inhibiting JAK3 in alopecia areata), and zanubrutinib (blocking BTK in mantle cell lymphoma). The most common mutant protein kinases in all cancers are the closely related EGFR and ErbB4 of the ErbB1/2/3/4 epidermal growth factor receptor family [3]. For a summary of the characteristics of small molecule protein kinase antagonists that were FDA-approved by 2023, see Refs. [2–4,17–21]. For a synopsis of drugs approved by the FDA and other international regulatory agencies, see Ref. [12]; the latter also includes information on the synthesis routes used during the discovery phase, many routes of which the authors obtained from patents.

Three of the non-FDA-approved drugs are used in the treatment of more than one disease. For example, apatinib is used for the treatment of gastric and non-small cell lung cancers, orelabrutinib is used for the management of mantle cell lymphoma, chronic lymphocytic leukemia, and small lymphocytic lymphoma. Of the 75 FDA-approved protein kinase blockers, nineteen are used in the treatment of more than one disease. Imatinib, for example, is approved for the treatment of eight distinct disorders. This medicinal inhibits the nonreceptor protein-tyrosine kinase Abl (and the BCR-Abl chimera – responsible for the pathogenesis of chronic myelogenous leukemia), Kit (the stem cell factor receptor), PDGFRα/β, Abl2, and epithelial discoidin domain-containing receptor-1 (DDR1) and receptor-2 (DDR2). DDR1/2, which are activated by collagen, participate in cell migration, proliferation, differentiation, and the remodeling the extracellular matrix. Imatinib is FDA-approved for (i) the first-line treatment of Philadelphia chromosome-positive chronic myelogenous leukemia, (ii) acute lymphoblastic leukemia, (iii) *KIT* mutation-positive gastrointestinal stromal tumors, (iv) myelodysplastic/myeloproliferative diseases with *PDGFR* gene-rearrangements, (v) dermatofibrosarcoma protuberans, (vi) hypereosinophilic syndrome, (vii) chronic eosinophilic leukemia, and (viii) as a second-line treatment for aggressive systemic mastocytosis without the KIT^{D816V} mutation [2,3]. Furthermore, imatinib is used off-label for the treatment of chordomas, desmoid tumors, advanced *KIT*-mutant melanomas, and

Table 2
Important residues in human ROCK1, JAK family, and BTK protein kinases.

	ROCK1	JAK1	JAK2	JAK3	TYK2	BTK	Inferred function
FERM domain		34–420	37–380	24–356	26–431		Interacts with receptor
SH2-like		439–544	410–482	375–475	450–529		Binds glutamate
Pseudokinase		583–855	545–809	521–781	589–875		Regulation
Kinase domain	76–338	875–1153	849–1124	822–1111	897–1176	402–655	Catalysis
Amino-terminal lobe							
Glycine-rich loop: GxGxΦG	^{83}GRGAFG^{88}	^{882}GEGHFG^{887}	^{856}GKGNFG^{861}	^{829}GKGNFG^{834}	^{904}GEGHFG^{909}	^{409}GTGQFG^{414}	Anchors ATP β-phosphate
β3-K (K of K/E/D/D)	K105	K908	K882	K855	K930	K430	Forms ion pair with ATP α- and β-phosphates
αC-E (E of K/E/D/D)	E124	E925	E898	E871	E947	E445	Forms ion pair with β3-K
Hinge residues	^{154}EYMPGGD^{160}	^{957}EFLPGSGS^{964}	^{930}EYKPYGS^{936}	^{903}EYLPSGC^{909}	^{979}EYVPLGS^{985}	^{475}EYMANGC^{481}	Connects N- and C-lobes
Carboxyterminal lobe							
Catalytic loop HR*D* (first *D* of K/E/*D*/D)	D198	D1003	D976	D949	D1023	D521	Catalytic base (abstracts proton)
Catalytic loop Asn (N)	N203	N1008	N981	N954	N1028	N526	Chelates Mg^{2+}(2)
Activation segment	216–244	1021–1051	994–1024	967–997	1041–1071	539–567	Positions protein substrate
AS *D*FG (second *D* of K/E/D/*D*)	D216	D1021	D994	D967	D1041	D539	Chelates Mg^{2+}(1)
AS phosphorylation site(s)	None	Y1034/Y1035	Y1007/Y1008	Y980/Y981	Y1054/Y1055	Y551	Stabilizes the AS after phosphorylation
APE, end of AS	^{242}SPE^{244}	^{1049}APE^{1051}	^{1022}APE^{1024}	^{995}APE^{997}	^{1069}APE^{1071}	^{565}PPE^{567}	Interacts with the αHI loop and stabilizes the AS
JH7		44–117	51–124	37–110	40–113		FERM domain
JH6		147–180	142–170	126–154	141–169		FERM domain
JH5		309–324	282–299	265–282	310–327		FERM domain
JH4		378–452	329–411	304–387	389–462		FERM + SH2 like
JH3		500–550	455–506	432–482	508–558		SH2 like
JH2		583–855	545–809	521–781	589–875		Pseudokinase
JH1		875–1153	849–1124	822–1111	897–1176		Protein-tyrosine kinase
No. of amino acids	1354	1153	1124	1111	1176	659	
UniProt KB ID	Q13464	P23458	O60674	P52333	P29597	Q06187	

[a]AS, activation segment; Φ, hydrophobic residue.

chronic myelogenous leukemia following allogeneic stem cell transplantation. Imatinib is thus a broad-spectrum inhibitor. Imatinib is a drug approved by regulatory agencies in China, Japan, South Korea, Europe and the United States.

2. Protein kinase structure

2.1. Primary, secondary, and tertiary structures

The newly approved drugs described in this review interact with several protein kinases including the ROCK protein-serine/threonine kinase, the JAK family of protein kinases, and the Bruton tyrosine kinase (BTK) so that the following description is generic. As first described for PKA (protein kinase A) by Knighton et al., protein kinases have a small N-terminal lobe and large C-terminal lobe (Fig. 1 A and 1D) [22]. The amino-terminal lobe is made up of a five-stranded antiparallel β-sheet (β1–β5) and a regulatory αC-helix that is observed in active and inactive orientations [23,24]. This small lobe contains a glycine-rich loop (GRL), sometimes called the P-loop (for the ATP phosphates), which links the N-lobe β1- and β2-strands; the loop contains GxGxΦG where the Φ denotes a hydrophobic residue. A valine that is two residues after the G-rich loop makes hydrophobic contact with the adenine portion of ATP as well as many small molecule protein kinase antagonists. Protein kinases contain an AxK sequence within the β3-strand and a conserved glutamate near the middle of the αC-helix. A salt bridge links the negatively charged αC-glutamate (E) and the positively charged β3-strand lysine (K) in catalytically competent protein kinases and such structures correspond to an "αC_{in}" conformation (Fig. 1 C). The αC_{in} conformation is necessary, but not sufficient, for the expression of full enzyme activity. Furthermore, the absence of this salt bridge indicates that the enzyme is catalytically inactive and the corresponding structure corresponds to the "αC_{out}" conformation (Fig. 1 F). The transition of the αC_{out} to the αC_{in} conformation is required for the expression of catalytic activity.

The carboxyterminal lobe is largely α-helical with eight conserved helices (αD–αI, αEF1, αEF2) [25]. The large lobe of catalytically active protein kinases also contains four short β-strands (β6–β9) (Fig. 1 A). The second residue of the β7-strand represents the floor of the adenine binding pocket and this residue interacts hydrophobically with all known ATP-competitive protein kinase inhibitors [26]. The large lobe contains a catalytic loop (CL) that catalyzes the transfer of the γ-phosphoryl group from ATP to the peptide/protein substrates. The carboxyterminal lobe also guides the peptide/protein substrate into the active site to enable catalysis.

Hanks and Hunter described 12 subdomains (I–VIa, VIb–XI) that comprise the operational components of protein kinases [27]. A K/E/D/D (Lys/Glu/Asp/Asp) tetrad plays a critical role responsible for the catalytic activity of all protein kinases. The *K* of the tetrad is the β3-strand lysine that forms salt bridges with the (i) αC-glutamate to form the αC_{in} structure (Fig. 1 C) and the (ii) α-phosphate and (iii) β-phosphate of ATP (not shown). Residues within the protein kinase activation segment position the phosphorylatable substrate into the active site. Furthermore, the HRD-aspartate of the catalytic-loop (the first *D* of the K/E/*D*/D tetrad) functions as a Lowry-Brönsted base (a proton acceptor). Madhusudan et al. hypothesized that the HRD-aspartate of the catalytic loop abstracts the proton from the protein substrate hydroxyl group [28]. Moreover, Zhou and Adams suggested that the HRD-aspartate positions the protein–OH group to promote the in-line nucleophilic attack of the oxygen with the γ-phosphate of ATP [29]. See Ref. [30] for a comprehensive summary of protein kinase enzymology and see Table 2 for a list of the important residues in protein kinases illustrated in this article.

The second *D* of the K/E/D/*D* tetrad is the first residue of the activation segment. This part of all protein kinases begins with DFG and ends with APE or a similar triad such PPE or SPE. Activation segments, which are about 35–40 residues long, are important regulatory and structural components of all protein kinases [31]. An HRD(x)$_4$N signature comprises the catalytic loop of functional protein kinases. The primary structure of the activation segment occurs carboxyterminal to the catalytic loop. Two Mg^{2+} ions – Mg^{2+}(1) and Mg^{2+}(2) – are essential

Table 3
Spine and shell residues of selected human protein kinase domains[a].

	Symbol	KLIFS No.	ROCK1	JAK1	JAK2	JAK3	TYK2	BTK
Regulatory spine residues								
β4-strand (N-lobe)	RS4	38	L139	Y940	Y913	Y886	Y962	L460
C-helix (N-lobe)	RS3	28	M128	L929	L902	L875	L951	M449
Activation loop DFG-F (C-lobe)	RS2	82	F217	F1022	F995	F968	F1042	F540
Catalytic loop HRD-H (C-lobe)	RS1	68	H196	H1001	H974	H947	H1021	H519
F-helix (C-lobe)	RS0	None	D260	D1063	D1036	D1009	D1083	D579
Shell residues								
Two residues upstream from the gatekeeper	Sh3	43	M151	L954	L927	L900	L976	I472
Gatekeeper, end of β5-strand	Sh2	45	M153	M956	M929	M902	M978	T474
αC-β4 loop	Sh1	36	V137	V938	V911	V884	I960	V458
Catalytic spine residues								
β3-AxK-A (N-lobe)	CS8	11	A103	A906	A880	A853	A928	A428
β2-strand (N-lobe)	CS7	15	V90	V889	V863	V863	V911	V416
β7-strand (C-lobe)	CS6	77	L205	L1010	L983	L956	L1030	L528
β7-strand (C-lobe)	CS5	78	L206	V1011	V984	V957	L1031	V529
β7-strand (C-lobe)	CS4	76	M204	V1009	I982	I955	V1029	C527
D-helix (C-lobe)	CS3	53	L161	L964	L937	L910	L986	L482
F-helix (C-lobe)	CS2	None	F267	T1070	V1043	S1012	T1090	L586
F-helix (C-lobe)	CS1	None	M271	L1074	L1047	V1016	L1094	I590

[a] From Refs. [34–36], https://klifs.net/, and https://www.uniprot.org/uniprotkb/.

for the activity of nearly all protein kinases. Mg^{2+}(1) interacts with the activation segment DFG-D and Mg^{2+}(2) interacts with the terminal catalytic loop asparagine (not shown).

The primary structure and length of the middle portion of the activation segment vary greatly among the members of the protein kinase superfamily [2]. The activation segment of nearly all members of the protein kinase superfamily contains one or more phosphorylatable residues. Moreover, activation segment phosphorylation is necessary for the expression of full enzyme activity in nearly all protein kinases. ErbB1/2/4 of the EGFR family are a noteworthy exception because they exhibit maximal activity in the absence of activation segment phosphorylation. The activation segment DFG occurs spatially near the conserved catalytic loop HRD and the N-terminus of the αC-helix. The regulatory αC-helix, which occurs within the small lobe, occupies a strategically important location between the two lobes. The protein kinase activation segment has an extended and open structure in the active form of all protein kinases (Fig. 1 A); in contrast it has a closed structure in most inactive kinases (Fig. 1D) [2]. The first two activation segment residues (DF) occur in different conformations. In active protein kinases, the DFG-D side chain points inward toward the ATP-binding site and it binds Mg^{2+}(1). This configuration is known as the "DFG-D_{in}" conformation (Fig. 1 C). In many inactive protein kinases, the DFG-D side chain points away from the ATP-binding site. This configuration is known as the "DFG-D_{out}" conformation (not shown). It is the property of DFG-D to bind (DFG-D_{in}) or not bind (DFG-D_{out}) Mg^{2+}(1) within the active site of the protein kinase that is important.

Modi and Dunbrack investigated the interaction of drugs with active and inactive conformations of protein kinases based upon the arrangement of the activation segment, which begins with the universal DFG sequence [32,33]. These authors found a collection of protein kinase conformations that depend on the location of the phenylalanine side chain (DFG-D_{in}, DFG-D_{out}, and DFG-$D_{intermediate}$) and the backbone dihedral angles of the xDF sequence where x is the residue proximal to the DFG signature. Modi and Dunbrack identified eight different conformations and classified them using the configuration (χ1) of the phenylalanine rotamer (minus, plus, trans) and on the Ramachandran regions (A, alpha; B, beta; L, left) of the xDF motif [33]. Their clusters divide the DFG-D_{in} configuration into six classes including BLAminus, which corresponds to active structures, and two common inactive forms, BLBplus and ABAminus. DFG-D_{out} structures occur mainly in the BBAminus conformation. The inactive conformations have features that block their interaction with Mg^{2+}, ATP, and/or their protein substrates. Modi and Dunbrack produced a searchable and noncommercial web site (http://dunbrack3.fccc.edu/kincore/) that allows one to establish whether a protein kinase conformation corresponds to an active enzyme (BLAminus) or to an inactive enzyme (other). We used this web site to determine whether the structures of our various drug-enzyme complexes correspond to active or dormant enzymes. See Refs. [2,32,33] for more information about these and related DFG activation segment arrangements.

2.2. Protein kinase hydrophobic spines

Kornev et al. evaluated the three-dimensional structures of active and dormant conformations of about two dozen protein kinases to identify important structural and functional residues [34,35]. Their analysis revealed a set of eight amino acids along with the adenine base of ATP that make up a C-spine (catalytic spine) and four amino acids that make up an R-spine (regulatory spine). These residues occur in both the amino-terminal and carboxyterminal lobes. These spines create a stable, but flexible, catalytically active ensemble. The C-spine positions ATP and the R-spine positions the protein substrate for catalysis. The R-spine contains residues from both the αC-helix and activation segment, whose conformations are important in producing active and inactive enzyme states. The exact alignment and positioning of both spines are necessary, but not sufficient, for the formation of catalytically competent protein kinases.

The R-spine contains the first residue of the β4-strand and the amino acid that is four residues N-terminal to the conserved αC-helix glutamate, both of which are within the amino-terminal lobe [34]. The R-spine also contains the HRD-histidine of the catalytic loop and the DFG-phenylalanine of the activation segment, both within the carboxyterminal lobe. The HRD-histidine N–H backbone forms a hydrogen bond with the carboxylate side chain of a conserved aspartate within the hydrophobic αF-helix. Meharena et al. labeled the R-spine residues as RS0, RS1, RS2, RS3, and RS4 from the bottom to the top [36]. We subsequently labeled the C-spine residues CS1–8 from the base to the apex (Fig. 1B/E) [26]. Note that the R- and C-spines of active protein kinases are linear (Fig. 1B). RS3 is displaced rightward in protein kinases with the αC_{out} structure (Fig. 1E). The identity of the C-spine, R-spine, and shell residues of the protein kinases considered in this article are listed in Table 3.

Based upon site-directed mutagenesis studies, Meharena et al. found three residues in murine protein kinase A that strengthen and stabilize the regulatory spine, which they identified as shell residues (Sh1, Sh2, and Sh3) (Fig. 1E) [36]. Their Sh1 mutant (V104G) had 5% of the

Table 4
Classification of small molecule protein kinase inhibitors[a].

Inhibitor type	Properties
I	Binds in and around the ATP-binding pocket of an active enzyme
I½ A/B	Binds in and around the ATP-binding pocket of an inactive DFG-D_{in} enzyme
I½ A	Extends into the back cleft
I½ B	Does not extend into the back cleft
II A/B	Bind in and around the ATP-binding site of an inactive DFG-D_{out} enzyme
II A	Extends into the back cleft
II B	Does not extend into the back cleft
III	Allosteric inhibitor bound next to the ATP-binding site
IV	Allosteric inhibitor bound away from the ATP-binding site
V	Bivalent inhibitor spanning two kinase domain regions
VI	Covalent inhibitor

[a] Adapted from Ref. [44].

catalytic activity of the wildtype enzyme and their M120G/M118G Sh2/Sh3 double mutant was devoid of catalytic activity. These results demonstrated that the shell residues support PKA catalytic activity. We hypothesize that the corresponding shell residues of all protein kinases play a similar activating role. The Sh1 residue is found within the section connecting the αC-helix with the β4-strand, the so-called back loop. The Sh2 residue (the gatekeeper) occurs at the end of the β5-strand immediately before the hinge and the Sh3 residue is found within the β5-strand two residues upstream from the Sh2 residue.

The gatekeeper controls access to a hydrophobic pocket contiguous with the adenine binding pocket [37,38], a pocket that interacts with many small molecule protein kinase antagonists. It is important to realize that many small molecule therapeutic steady-state ATP-competitive protein kinase inhibitors interact with the C-spine (CS6/7/8), shell (Sh1 and Sh2) residues, and the R-spine (RS2/3). Ung et al. found that approximately one quarter of protein kinases has a small gatekeeper residue (e.g., Thr, Val) and about three quarters have a relatively large gatekeeper residue (e.g., Met, Leu, Phe) [39]. Also of importance for long-term drug efficacy, the gatekeeper residue of drug target protein kinases is one of the more common sites of drug-resistant mutation [3,40].

3. Classification of protein kinase-inhibitor complexes and a description of inhibitor-binding pockets

Based upon earlier findings [38,41–43], we classified the small molecule protein kinase inhibitors into seven main groups that include reversible (Groups I, I½, II, III, IV, and V) and irreversible inhibitors (VI) as noted in Table 4. We divided the type I½ and type II antagonists into A and B subtypes [44]. Subtype A drugs extend past the gatekeeper residue into the back cleft. In contrast, subtype B drugs are those that do not extend into the back cleft. Subtype A inhibitors generally have longer residence times than Subtype B blockers.

We followed the lead of Liao, van Linden et al., Kooistra et al., and Kanev et al. [43,45–47] in defining the drug-binding pockets. An illustration depicting the location of the pockets and subpockets is provided in Fig. 2. The region between the amino-terminal and carboxyterminal lobes is divided into a front cleft or front pocket, a gate area, and a back cleft. The front pocket contains the hinge, the linker residues that connect the hinge residues to the αD-helix in the C-terminal lobe, the glycine-rich loop (GRL), the adenine-binding pocket (AP), and the catalytic loop ($HRD(x)_4N$). The back pocket (hydrophobic pocket II, or HPII) includes the gate area and the neighboring back cleft. The location of the front cleft, gate area, and back cleft within the JAK2 protein kinase domain is depicted in Fig. 2B.

Kanev et al. [47] and van Linden et al. [45] described the mode of drug and ligand binding to more than 5200 human and mouse protein kinases. Their KLIFS (kinase–ligand interaction fingerprint and structure) listing includes an alignment of 85 ligand binding-site residues that are found in both the N-terminal and C-terminal lobes; their catalogue facilitates a comparison of ligands and drugs based upon their binding characteristics. Such information provides a means to detect common and unique drug-enzyme interactions. These investigators formulated a canonical amino acid residue numbering system that facilitates the comparison of different protein kinases and their ligands. Table 3 indicates the relationship of the C-spine, R-spine, and shell amino acid residue numbering system and the KLIFS database nomenclature and Fig. 3 illustrates the location of the KLIFS residues within the protein kinase domain. These authors established a valuable noncommercial and searchable web site, which is regularly updated, that provides comprehensive information on the interaction of protein kinases with drugs and ligands (klifs.net).

The Blue Ridge Institute for Medical Research (BRIMR) maintains a

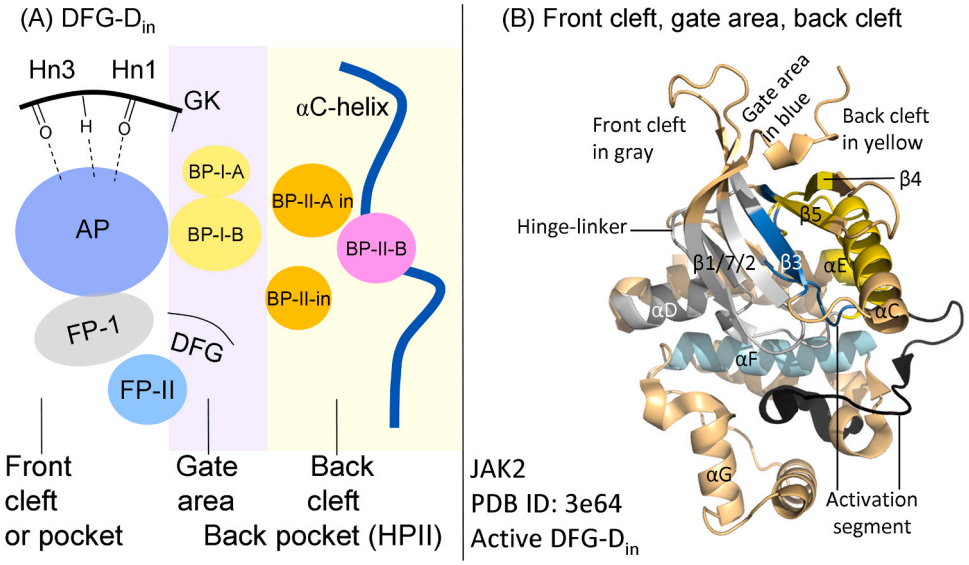

Fig. 2. (A) Location of the protein kinase domain drug-binding pockets in the DFG-D_{in} enzyme form. (B) Location of the protein kinase front cleft, gate area, and back cleft. AP, adenine pocket; BP, back pocket; FP, front pocket; Hn, hinge; HPII, hydrophobic pocket II; GK, gatekeeper.
Adapted from Refs. [43,45–47].

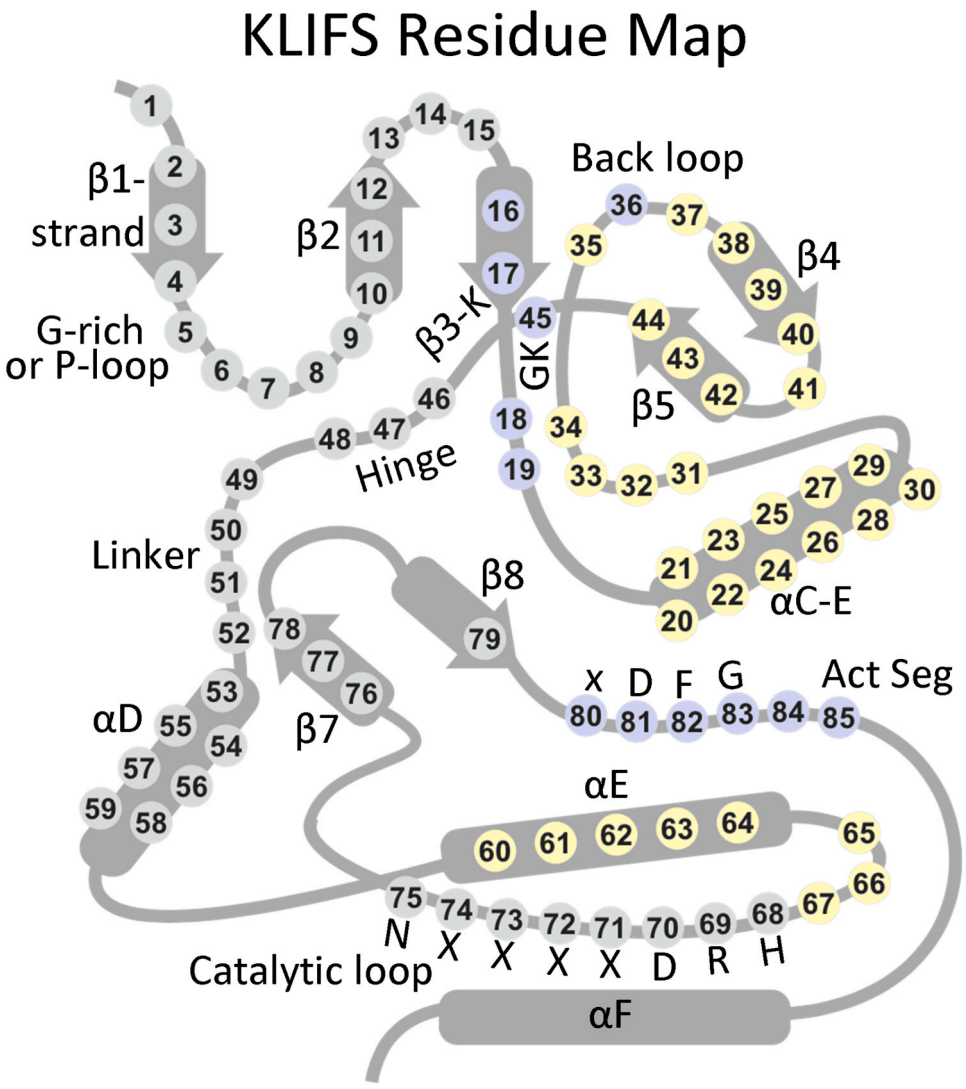

Fig. 3. The location of the KLIFS residues within a generic protein kinase domain. The gray residues correspond to the front cleft; blue, gate area; yellow, back cleft. Act Seg, activation segment.

web site that depicts the FDA-approved protein kinase inhibitors and provides their (i) molecular structures, (ii) the number of hydrogen bond donors/acceptors, (iii) the Log of the partition and distribution coefficients, (iv) the number of rotatable bonds and rings, (v) the year of initial approval, (vi) their main protein kinase targets, and (vii) their therapeutic indications. The website also provides a link to the corresponding FDA labels. This website, which is found at www.brimr.org/PKI/PKIs.htm, is updated following FDA-approval of new protein kinase antagonists. The website contains Excel files that can be downloaded and used for determining means, ranges, and ranking various parameters. The BRIMR website does not contain information on drugs approved by non-FDA regulatory agencies. Carles et al. maintain a web site (PKIDB) that includes a comprehensive catalogue of protein kinase blockers that are in clinical trials or that have been approved by the FDA or other international regulatory agencies [6]. Their website is searchable, noncommercial, and is regularly updated and includes the physical properties and structures of the various drugs, their protein kinase targets, their medicinal indications, the year of first approval by regulatory agencies (if applicable), trade names, smiles codes, and a summary of pdf files of X-ray structures (http://www.icoa.fr/pkidb/). The PKIDB also contains links for each of the drugs to ChEMBL, PubChem, DrugBank, and other data bases. See Ref. [48] for additional information on the interactions of small molecule protein kinase inhibitors with their associated enzymes.

4. Small molecule protein kinase inhibitors approved outside of the United States

4.1. Fasudil, a ROCK and Rho antagonist

Fasudil is an isoquinoline derivative (Fig. 4A) that was approved in Japan and China for the treatment of vasospasm in patients with subarachnoid hemorrhage in 1995 and 2010, respectively. This agent was discovered by investigators seeking calcium blockers for the treatment of this disorder [8–10,49]. However, experiments indicated that fasudil functions as a ROCK protein kinase antagonist thus becoming the first small molecule kinase inhibitor to be approved by a regulatory agency. This medicinal is not approved by the FDA. Rho-associated coiled-coiled-containing kinases (ROCKs) were initially described as downstream effectors of the small GTP-binding protein Rho. ROCK belongs to the serine/threonine AGC (cAMP-dependent protein kinase/protein kinase G/protein kinase C) family, the inhibition of which influences the functions of many downstream substrates. ROCK is expressed as two isoforms, ROCK1 (also known as ROCKβ, ROCK I, Rhokinase β, or p160ROCK) and ROCK2 (also called ROCKα, ROCKII, or Rho kinase), both of which have a molecular weight of approximately 160 kDa.

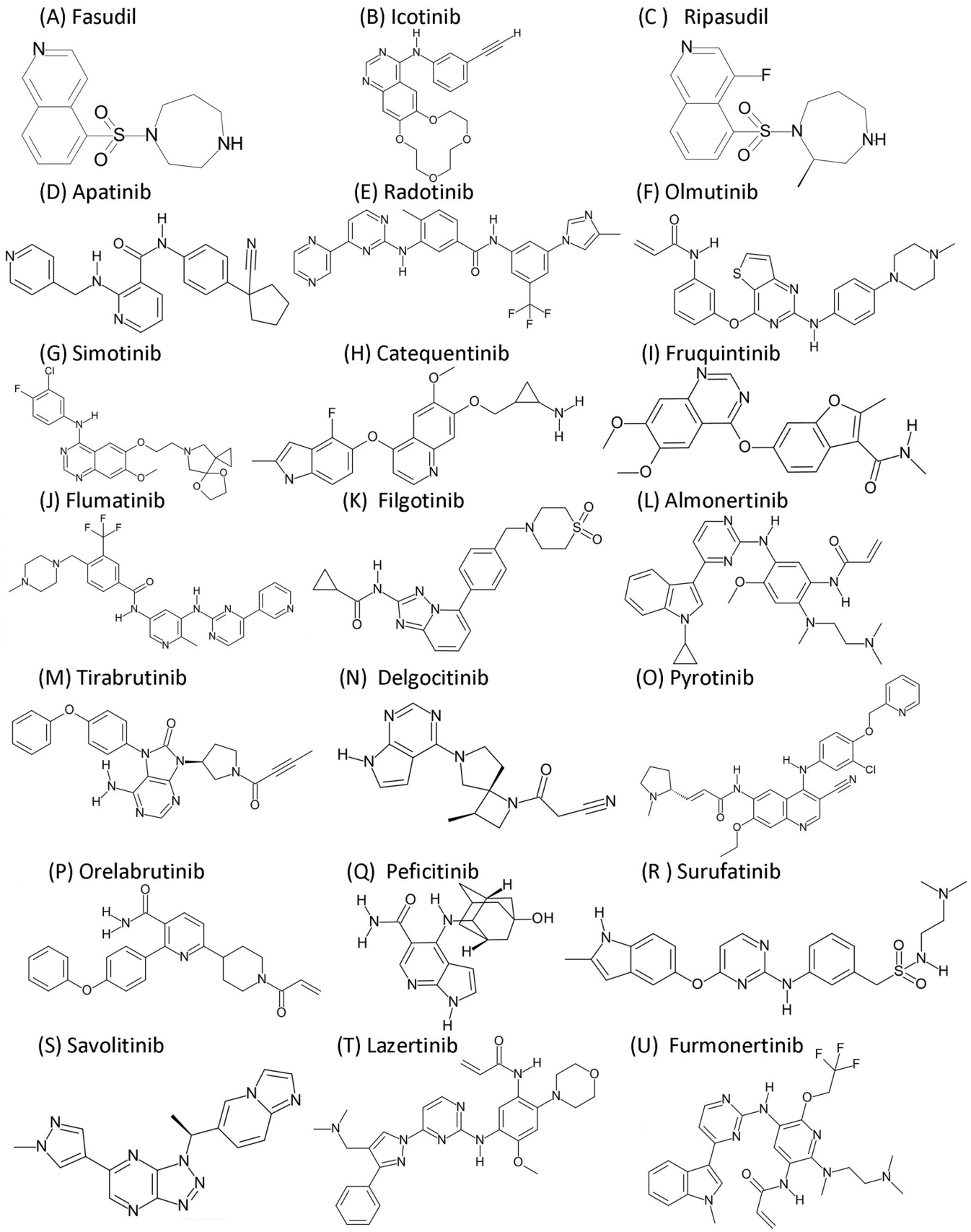

Fig. 4. Structures of the 21 drugs approved by international regulatory agencies.

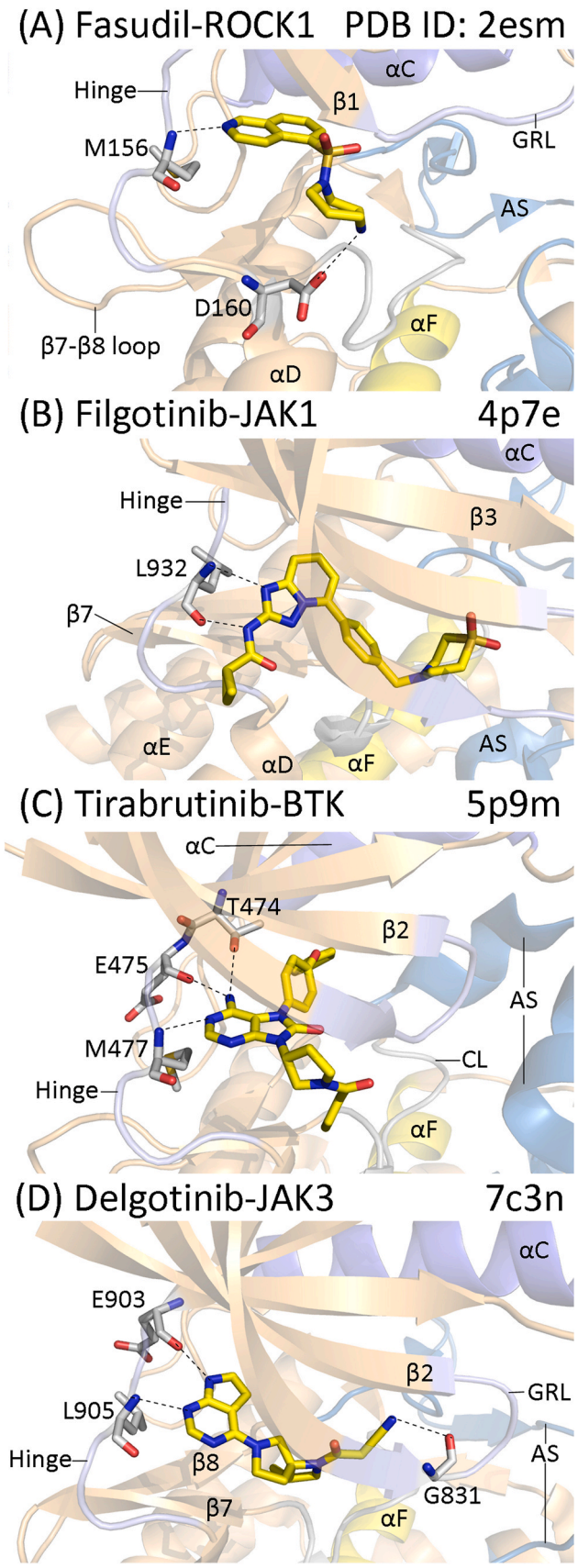

Fig. 5. Drug-enzyme complexes. AS, activation segment; CL, catalytic loop; GRL, glycine-rich loop. Dashed lines represent polar bonds.

ROCK1 and ROCK2 are widely expressed in embryonic and adult tissues. Compared to ROCK1, which is universally expressed, ROCK2 is found predominantly in brain, heart, lung, and muscle (especially smooth muscle). ROCK1/2 regulate the activity of muscle myosin regulatory light chain proteins by direct phosphorylation and by phosphorylation and inhibition of the myosin binding subunit of myosin phosphatase. The ROCK family participates in cytoskeletal rearrangement, cell adhesion, and stress fiber formation. Furthermore, ROCK resides mainly in the cytoplasm, with lesser amounts in the nucleus and cell membrane. For a summary of the properties of ROCK enzymes, see Refs. [50–53].

ROCK1 contains a protein kinase domain (residues 76–338), a long coiled-coil domain (425–1100), and a pleckstrin homology domain (1103–1239). Under basal conditions, ROCK exists in an autoinhibited state [54]. The coiled-coil domains and the pleckstrin homology domain inhibit catalytic activity by binding to the protein kinase domain. When Rho-GTP binds to the Rho-binding region of the coiled-coiled domain, the interactions between the protein kinase domain and the C-terminal region are disrupted allowing for catalytic activity.

The IC_{50} value of fasudil for ROCK1 is about 530 nM [54] and this is a very low potency for an approved protein kinase blocker. Jacobs et al. [54] determined the X-ray structure of fasudil bound to human ROCK1 and they observed that the *N*1 of isoquinoline forms a hydrogen bond with the backbone N–H group of M156, the third hinge residue. The N–H group of homopiperazine hydrogen bonds with the side chain of D160, the last residue in the hinge-linker segment (Fig. 5A). The drug makes hydrophobic contact with the first two shell residues (Sh1/2), three catalytic spine residues (CS6/7/8) and the Klifs residue-3 (Table 5). The Klifs-3 residue is found immediately before the G-rich loop and it interacts with a large number of small molecule protein kinase antagonists. Fasudil also interacts hydrophobically with M153 (the gatekeeper), E154, Y155, M156, and D160 of the hinge-linker segment, and A215 (the x residue of xDFG). Modi and Dunbrack [33] found that this enzyme form occurs within the BLAminus enzyme cluster, which indicates that the enzyme is in an active conformation. The drug occupies the front pocket (Klifs.net) and we and Modi and Dunbrack label fasudil with ROCK1 as a type I inhibitor [33,44]. Fasudil is listed in 14 clinical trials (www.clinicaltrials.gov) of which five have been completed (Table 6). See Refs. [8,10] for findings of clinical trials involving this medicine.

4.2. *Icotinib, an EGFR family blocker*

Icotinib is a quinazoline derivative (Fig. 4B) that was approved in China for the treatment of NSCLC in 2012 [55]. This medicinal blocks EGFR and several of its mutants. The EGFR family is among the most investigated receptor protein-tyrosine kinases owing to this family's general role in signal transduction and in oncogenesis [56–59]. This receptor family consists of four members that belong to the ErbB lineage of proteins (ErbB1–4). The ErbB proteins operate as homo and heterodimers. These receptors possess an extracellular domain that consists of four components: domains I and III are leucine-rich sections that participate in growth factor binding (except for ErbB2) and domains II and IV possess multiple disulfide bonds. Furthermore, domain II participates in both homodimer and heterodimer formation within the ErbB/HER family of proteins, where HER denotes Human Epidermal growth factor Receptor. Seven ligands bind to EGFR: epidermal growth factor (EGF), transforming growth factor-α (TGFα), amphiregulin (AR), epigen (EPG), betacellulin (BTG), heparin-binding epidermal growth factor like (HB-EGF), and epiregulin (EPG); none bind to ErbB2; two bind to ErbB3: Neuregulin1/2 (NR1/2); and seven ligands bind to ErbB4: BTC, EPR, HB-EGF, and NRG1/2/3/4. The extracellular domain is followed by a single transmembrane segment with about 25 amino acid residues and an intracellular portion of approximately 550 amino acid residues that contains (i) a short juxtamembrane portion, (ii) a protein kinase domain, and (iii) a carboxyterminal tail. ErbB2 lacks a known activating ligand and ErbB3 is kinase impaired; despite these

Table 5
Human enzyme-drug hydrophobic (Φ) interactions based upon their common KLIFS residue numbers[a]

	PDB ID	RS1/2/3/4	Sh1	Sh2	Sh3	CS5	CS6	CS7	CS8	Klifs-3[b]	KLIFS pockets[a]
KLIFS no. →		68/82/28/38	36	45	43	76	77	11	15	3	
Drug-enzyme ↓											
Type I inhibitors											
Fasudil-ROCK1	2esm		Φ	Φ			Φ	Φ	Φ	Φ	F
Peficitinib-JAK2	6aaj		Φ	Φ			Φ	Φ	Φ	Φ	F, FP-I
Peficitinib-JAK3	6aak		Φ	Φ			Φ	Φ	Φ	Φ	F, FP-I
Peficitinib-Tyk2	6aam		Φ	Φ			Φ	Φ	Φ	Φ	F, FP-I
Type I½ A inhibitor											
Tirabrutinib-BTK	5p9m	0/Φ/Φ/0	Φ	Φ	Φ	Φ	Φ	Φ	Φ	Φ	F, G, B, BP-I-B
Type I ½ B inhibitors											
Filgotinib-JAK1	4p7e		Φ	Φ			Φ	Φ	Φ	Φ	F, FP-II
Delgotinib-JAK3	7c3n		Φ	Φ			Φ	Φ	Φ	Φ	F, FP-I/II
Peficitinib-JAK1	6aah		Φ	Φ			Φ	Φ	Φ	Φ	F, FP-I

[a] klifs.net.
[b] KLIFS-3, kinase-ligand interaction fingerprint and structure residue-3.

Table 6
Clinical Trial Information (www.clinicaltrials.gov).

Drug	No.	No. complete	Diseases under investigation
Fasudil	14	5	Amyotrophic lateral sclerosis, retinopathy, various cardiovascular conditions
Icotinib	101	19	Lung, esophageal, pancreatic, and breast cancers, psoriasis
Ripasudil	14	3	Glaucoma, Fuchs endothelial corneal dystrophy, chronic obstructive pulmonary disease
Apatinib or rivoceranib	479	63	CRC, NSCLC, gastric, liver, breast, and cervical cancers, sarcoma, many other tumor types
Radotinib	7	2	Parkinson disease, leukemia
Olmutinib	7	6	NSCLC
Simotinib	2	1	NSCLC
Catequentinib	344	29	Cervical, breast, liver, esophageal, thyroid, and renal cell cancers, NSCLC, and sarcomas
Fruquintinib	82	15	CRC, NSCLC, gastric and renal cell carcinomas, advanced solid tumors,
Flumatinib	14	1	AML, ALL, CML
Filgotinib	53	29	Ulcerative colitis, Crohn disease, rheumatoid arthritis, psoriatic arthritis
Almonertinib	49	2	NSCLC, advanced malignancies, lung adenocarcinoma
Tirabrutinib	11	6	CLL, rheumatoid arthritis, B cell lymphoma, Sjögren syndrome
Delgocitinib	14	9	Atopic dermatitis, eczema, discoid lupus erythematosus
Pyrotinib	159	12	Breast and gastric cancers, $HER2^+$ solid tumors, CRC
Orelabrutinib	36	2	B cell lymphoma, mantle cell lymphoma, systemic lupus erythematosus, relapsing-remitting multiple sclerosis
Peficitinib	34	33	Rheumatoid arthritis, psoriasis, ulcerative colitis
Surufatinib	66	15	Neuroendocrine tumors, CRC, sarcomas, gastric adenocarcinoma, and biliary tract, ovarian, breast, liver, and thyroid cancers
Savolitinib	41	15	Solid tumors, NSCLC, CRC, renal cell and, prostate cancers
Lazertinib	33	8	NSCLC, advanced tumors,
Fumonertinib	32	2	NSCLC, lung adenocarcinoma

properties, the ErbB2–ErbB3 heterodimer complex is the most active dimer in the family. These receptors are implicated in the pathogenesis of a large proportion of lung and breast cancers, which rank first and second, respectively, in the incidence of all types of cancers (excluding skin) worldwide [60]. About 20% of non-small cell lung cancers possess activating mutations in *EGFR*. Greater than 90% of these individuals have exon-19 deletions (^{746}ELREA^{750}) or the exon-21 L858R substitution.

Icotinib has an IC_{50} value in the single-digit nanomolar range against EGFR (5 nM) and it also inhibits its L858R, L861Q, T790 M, and T790M/L858R mutants [61]. Icotinib does not significantly inhibit any other kinase from a panel of 88 related protein kinases and it displays a broad-spectrum of antitumor activity, especially on tumor cell lines with high expression levels of EGFR. This agent is listed in 101 clinical trials of which 19 have been completed (Table 6). See Refs. [62,63] for a summary of clinical trials that led to its approval.

4.3. Ripasudil, a ROCK and Rho inhibitor

Ripasudil is an isoquinoline derivative (Fig. 4C) and it was approved in Japan for the treatment of glaucoma in 2014 [64]. Of the 21 drugs approved outside of the United States that are considered in this article, ripasudil is an eyedrop and delgocitinib is a topical cream and all of the others are orally bioavailable. Unlike fasudil, the quinoline in ripasudil contains a fluorine group and the homopiperazine is methylated. The IC_{50} of ripasudil for ROCK1 is 51 nM and that for ROCK2 is 19 nM [65]. Ripasudil is listed in 14 clinical trials of which three have been completed. Besides glaucoma, one trial is focused on retinopathy of prematurity, another with chronic obstructive pulmonary disease, and a number involve Fuchs endothelial corneal dystrophy (Table 6). Some of the properties of ROCK1/2 are given in Section 4.1; we lack X-ray structures of ripasudil bound to either ROCK1 or ROCK2. See Refs. [66,67] for a summary of the clinical trials that led to the approval of ripasudil in Japan.

4.4. Apatinib, a VEGFR antagonist

Apatinib (rivoceranib) is a pyridinecarboxamide (Fig. 4D) that was approved in China for the treatment of gastric cancer and NSCLC in 2014. This drug blocks the VEGFR family of receptor protein-tyrosine kinases. This family of enzymes is a common target of protein kinase inhibitors owing to their role in vasculogenesis and angiogenesis [68–70]. Vascular endothelial cells are usually quiescent in adult humans and they are long lived and divide less than once per decade. When tumors reach a size of 0.2–2.0 mm in diameter, they become hypoxic and limited in size in the absence of angiogenesis. There are approximately 30 endogenous pro-angiogenic factors and a similar number of anti-angiogenic factors. In order for further growth to occur, tumors undergo an angiogenic switch where the action of pro-angiogenic factors prevails, resulting in angiogenesis and tumor progression. A major mechanism for promoting angiogenesis results from the increased production of vascular endothelial growth factors (VEGF) following the up-regulation of the hypoxia-inducible transcription factor. The human VEGF family consists of VEGF (VEGF-A), VEGF-B, VEGF-C, VEGF-D, and placental growth factor (PlGF). There are

three VEGF receptors (VEGFR1/2/3) that cooperate to promote vasculogenesis and angiogenesis. These receptors regulate vascular endothelial cell growth, permeability, migration, and survival. VEGFR2 and VEGFR3 stimulate endothelial cell growth by activating the PI 3-kinase/AKT and MAP kinase pathways. Owing to the importance of angiogenesis in tumor progression, inhibition of VEGFRs represents an attractive cancer treatment. Tian reported that the apatinib IC_{50} value for VEGFR2 was 1 nM and that for VEGFR1 was 70 nM [71]. This agent is under study in 479 clinical trials (all in China) of which 63 are completed (Table 6). Nearly all of the trials are directed toward solid tumors, both sarcomas and carcinomas. See Refs. [72,73] for studies on the mechanism of action of apatinib and Ref. [74] for a summary of the clinical trials of this agent in patients with breast cancer.

4.5. Radotinib, a BCR-Abl blocker

Radotinib is a pyrazine-pyrimidine benzamide derivative (Fig. 4E) that was approved in South Korea for the treatment of chronic myelogenous leukemia (CML) in 2015. This leukemia is an indolent malignant hematological ailment that accounts for about 15% of all leukemia cases. This condition results from the creation of the Philadelphia chromosome that involves a reciprocal translocation that produces a shortened chromosome 22 and a lengthened chromosome 9 – the Philadelphia chromosome [2,75,76]. As a result of this translocation, a dysregulated BCR-Abl fusion oncoprotein is formed and it results in the abnormal proliferation of white blood cells. The treatment of CML with imatinib revolutionized the management of this illness and prompted the discovery and development of dozens of orally effective protein kinase inhibitors that are used in the treatment of several neoplastic and immunologic illnesses [3,75,76]. The BCR-Abl fusion protein lacks the physiological N-terminal myristoyl group that binds to a hydrophobic pocket in the large protein kinase lobe and that inhibits enzyme activity. The absence of the myristoyl group leads to enhanced protein kinase catalytic activity. Kim et al. reported that the IC_{50} of radotinib for wildtype Abl is about 34 nM [77]. Radotinib is undergoing studies in seven clinical trials of which two are completed (Table 6). In addition to CML, one trial is examining the efficacy of radotinib in the treatment of Parkinson disease. See Refs. [78–80] for additional information on the pharmacology of radotinib and its performance in clinical trials.

4.6. Olmutinib, an epidermal growth factor receptor (EGFR) inhibitor

Olmutinib is an orally bioavailable anilinothienopyrimidine derivative (Fig. 4F) that was approved in South Korea (2016) for the treatment of patients with locally advanced or metastatic NSCLC whose tumors harbor *EGFR-T790M* mutations, who had been previously treated unsuccessfully with an EGFR tyrosine kinase inhibitor [81]. Olmutinib potently inhibits EGFR in HCC827 cells expressing *EGFR DEL19* (IC_{50} value of 9.2 nM) and H1975 cells expressing *EGFR L858R/T790M* (IC_{50} value of 10 nM). In contrast, the IC_{50} of olmutinib against cells expressing wildtype EGFR is 2225 nM [81]. The properties of the EGF and EGFR family are given in Section 4.2. Only seven clinical trials are associated with olmutinib of which six are completed (Table 6). We lack the X-ray crystal structure of olmutinib with wildtype or mutant EGFRs. However, it can be classified as a type VI inhibitor owing to the formation of a covalent bond [44] with C797 or the comparable residue in the mutant enzymes. See Refs. [82,83] for the results of clinical trials involving olmutinib.

4.7. Simotinib, an EGFR antagonist

Simotinib is a methoxyquinazoline-4-amine derivative (Fig. 4G) that was approved in China for the treatment of solid tumors in 2018. Based upon its structure, it is not a covalent inhibitor. There is little information on this EGFR inhibitor in the public domain. Two clinical trials with simotinib are listed at www.clinicaltrials.gov and one is completed. For a summary of a phase I clinical trial, see Ref. [84].

4.8. Catequentinib, a VEGFR blocker

Catequentinib (anlotinib) is a methoxyquinoline-indole derivative (Fig. 4H) that was approved in China in 2018 for the treatment of patients with locally advanced or metastatic NSCLC who have undergone progression or recurrence after $\geq$ 2 lines of systemic chemotherapy [85]. This medicinal is a VEGFR2 inhibitor with an IC_{50} value of 0.2 nM and a VEGFR3 IC_{50} value of 0.7 nM [86]. Catequentinib is an orally bioavailable small molecule that also inhibits FGFR1/2/3/4, PDGFRα, RET (rearranged during transfection), and the stem cell factor receptor (Kit) [87]. It is likely that inhibition of these receptors plays a part in both the therapeutic efficacy of catequentinib as well as its toxicity. The role of the VEGF and VEGFR families in vasculogenesis, angiogenesis, and tumor progression is described in Section 4.4. Catequentinib efficacy is or has been under investigation in 344 clinical trials of which 29 have been completed (Table 6). This medicine has encouraging efficacy and a manageable and tolerable safety profile in a broad range of malignancies, including renal cell cancer, medullary thyroid cancer, gastric cancer, and esophageal squamous cell carcinoma [87,88].

4.9. Fruquintinib, a VEGFR2 inhibitor

Fruquintinib is a dimethoxyquinazoline derivative (Fig. 4I) that was approved in China in 2018 for the treatment of metastatic colorectal cancer in people who have undergone at least two prior lines of chemotherapy with fluoropyrimidine, oxaliplatin, and irinotecan [89]. Colorectal cancer (CRC) is the fifth most common tumor with approximately 1.1 million cases worldwide and it is the fourth leading cause of cancer-related mortality worldwide with about 580,000 deaths in 2020 [60]. This orally effective agent inhibits VEGFR1/2/3 with IC_{50} values of 33 nM, 35 nM, and 0.5 nM, respectively [90]. The compound also has weak activity against RET, FGFR-1 and the Kit receptor protein-tyrosine kinases. In addition, preclinical studies show that fruquintinib inhibits endothelial cell proliferation and tubule sprouting, thereby preventing tumor angiogenesis. The efficacy of this medicine is or has been investigated in the treatment of CRC and other solid tumors in 82 clinical trials of which 15 have been completed (Table 6). For a summary of these and other clinical trials involving fruquintinib, see Refs. [89,90].

4.10. Flumatinib, a BCR-Abl antagonist

Flumatinib is a trifluormethylbenzamide derivative (Fig. 4J) that was approved in China for the treatment of Philadelphia-chromosome positive chronic myelogenous leukemia in 2019 [91]. This compound is a powerful inhibitor of BCR-Abl (IC_{50} value of 1.2 nM) and a weaker inhibitor of PDGFRβ (IC_{50} of 308 nM) and Kit (IC_{50} of 666 nM) [92]. For a description of the role of BCR-Abl in the pathogenesis of CML, see Section 4.5. The efficacy of this medicine is or has been investigated in the treatment of CML and ALL in 14 clinical trials of which one has been completed (Table 6). For a summary of these and other clinical trials, see Refs. [91,93].

4.11. Filgotinib, a JAK blocker

Filgotinib is a triazolo[1,5-*b*]pyridine derivative (Fig. 4K) that was approved in Japan for the treatment of rheumatoid arthritis in 2020 [94]. This compound inhibits JAK family members with IC_{50} values of 10 nM, 25 nM, 150 nM, and 79 nM against JAK1, JAK2, JAK3, and TYK2, respectively (Klifs.net). Each of these nonreceptor protein-tyrosine kinases contains a JAK homology pseudokinase (JH2) domain that regulates the adjacent protein kinase domain (JH1). JAK1/2 and TYK2 are ubiquitously expressed whereas JAK3 is found predominantly in hematopoietic cells [95,96]. This enzyme family is regulated by numerous cytokines including interferons, interleukins,

and hormones (thrombopoietin, erythropoietin, and growth hormone). Ligand binding to cytokine and hormone receptors leads to the activation of their associated Janus kinases, which then catalyze the phosphorylation of the receptors. The SH2 domain of STATs (signal transducers and activators of transcription) binds to the receptor phosphotyrosine residues thus promoting STAT phosphorylation by the Janus kinases and consequent activation. Active STAT dimers are translocated into the nucleus where they participate in the regulation of the expression of hundreds of proteins. JAK-STAT dysregulation leads to autoimmune disorders such as rheumatoid arthritis, ulcerative colitis, and Crohn disease. JAK-STAT dysregulation also plays a role in the pathogenesis of myelofibrosis, polycythemia vera, and other myeloproliferative illnesses. JAK1 and JAK3 signaling participate in the pathogenesis of inflammatory ailments while JAK1 and JAK2 signaling are involved in the pathogenesis of several malignancies including lymphomas and leukemias as well as myeloproliferative neoplasms.

Menet et al. determined the X-ray crystal structure of filgotinib bound to human JAK1 [97] and they observed that the drug hydrogen-bonded to the backbone N–H and C═O groups of the third-hinge residue (E932) (Fig. 5B). The drug interacts hydrophobically with two shell residues (Sh1/2), three catalytic spine residues (CS6/7/8), and the Klifs-3 residue (Table 5). Filgotinib also makes hydrophobic contact with G856, K857, and G861 of the G-rich loop, S862 of the β2-strand, K882 of the β3-strand, M929 (the gatekeeper), along with E930, Y931, L932, P933, Y935, and G935 of the hinge-linker segment, G993 (the x of xDFG), and DFG-D994. The drug occupies the front pocket and FP-II (Klifs.net). JAK1 has the inactive ABAminus conformation as defined by Modi and Dunbrack [33]. We therefore classify filgotinib as a type I½ B inhibitor because the enzyme is an inactive DFG-D_{in} and αC_{in} conformation and the drug does not extend into the back pocket [44]. The drug is listed in 53 clinical trials of which 29 are completed (Table 6). See Ref. [94] for a summary of the clinical trials that led to its approval.

4.12. Almonertinib, an EGFR inhibitor

Almonertinib (aumolertinib) is an indole-pyrimidine derivative (Fig. 4L) that is approved in China (2020) as a second-line treatment for patients with metastatic *EGFR T790M* mutant NSCLC [12]. Almonertinib demonstrated powerful EGFR mutant inhibitory activity against the *T790M*, *del19/T790M* and *L858R/T790M* mutants (concentration that inhibits 50%: 0.37, 0.21, and 0.29 nM, respectively), but was less effective against wildtype EGFR (IC_{50} value of 3.4 nM) [98]. See Section 4.2 for a description of the actions of the EGFR family. The efficacy of this medicine is or has been investigated in 49 clinical trials of which two have been completed (Table 6). We lack the X-ray structure of this compound bound to its cognate enzyme. However, we classify it as a type VI inhibitor because it forms a covalent bond with its target [44]. See Ref. [99] for information on clinical trials involving almonertinib.

4.13. Tirabrutinib, a BTK antagonist

Tirabrutinib is a phenoxyphenyl-purine derivative (Fig. 4M) that was approved in Japan (2020) for the treatment of patients with recurrent or refractory primary central nervous system lymphomas [100]. Later that year, the drug received additional approval for the treatment of Waldenström macroglobulinemia and lymphoplasmacytic lymphoma [101]. The IC_{50} value of the drug for BTK is 6.8 nM [102]. The Bruton nonreceptor protein-tyrosine kinase (BTK), a deficiency of which leads to X-linked agammaglobulinemia, plays an essential role in B cell antigen receptor signaling. [103]. Because of the exclusivity of this protein in B cells, the BTK acronym could represent B cell Tyrosine Kinase. The domains of BTK include a PH (pleckstrin homology) domain that interacts with membrane-associated phosphatidylinositol trisphosphate, a TH (TEC homology) domain, which is followed by an SH3, SH2, and finally a protein kinase domain. BTK is activated by the SYK (spleen tyrosine kinase) and Lyn (a Src family member) protein kinases following B cell receptor activation. SYK attracts and activates PI3 kinase-δ, which catalyzes the conversion of membrane-associated phosphatidylinositol 4,5 bis-phosphate (PIP_2) to phosphatidylinositol 3,4, 5-trisphosphate (PIP_3). The amino-terminal PH lipid-interaction module of BTK is attracted to PIP_3 thereby allowing SYK and Lyn to catalyze the trans-phosphorylation of BTK at Tyr551 within the activation segment resulting in enzyme activation. The attraction of BTK dimers to PIP_3 molecules within the membrane can also result in activation segment trans-autophosphorylation and activation. BTK in turn mediates the phosphorylation and activation of phospholipase Cγ2. PLCγ2 catalyzes the hydrolysis of PIP_2 to generate inositol trisphosphate (IP_3) and diacylglycerol (DAG). IP_3 releases Ca^{2+} from intracellular stores. In turn, DAG and Ca^{2+} activate PKCβ, which leads to the activation of the Ras/RAF/MEK/ERK signaling module that promotes cell growth and proliferation [104–109]. Both pathways contribute to the maturation of antibody-producing B cells. Dysregulation of B cell receptor signaling occurs in several B cell neoplasms such as chronic lymphocytic leukemia, mantle cell lymphoma, and Waldenström macroglobulinemia.

Bender et al. determined the X-ray crystal structure of tirabrutinib bound to BTK [110]. They found that the drug forms hydrogen bonds with the (i) sidechain of T474 (the gatekeeper residue), (ii) the C═O backbone of E475 (the first hinge residue), and (iii) the N–H group of M477 (the third hinge residue) (Fig. 5C). The drug also makes hydrophobic contact with the three shell residues (Sh1/2/3), two R-spine residues (RS2/3), four catalytic spine residues (CS5/6/7/8), and KLIFs-3 residue (Table 5). The drug also interacts hydrophobically with T410 and G411 of the G-rich loop, K436 of the β3-strand, Y476, M477, and C481 of the hinge-linker segment, R525 and N526 of the catalytic loop, S538 (the x of xDFG), DFG-D539 of the activation segment, and L542 of the catalytic loop. The drug occurs in the front pocket, gate area, back pocket, and BP-I-B (Klifs.net). Modi and Dunbrack classify the drug as a type 1.5_Back antagonist with an inactive BLBplus conformation [33]. The enzyme assumes an inactive DFG-D_{in} and αC_{out} conformation and the drug extends into the back cleft; the drug is thereby classified as a type I½ A inhibitor [44]. A total of 11 clinical trials with seven completed are listed for tirabrutinib (Table 6). See Refs. [111,112] for a summary of clinical trials involving tirabrutinib.

4.14. Delgocitinib, a JAK blocker

Delgocitinib is a pyrrolo[2,3-*d*]pyrimidine derivative (Fig. 4N) that was approved in Japan (2020) for the topical treatment of atopic dermatitis [113]. The drug is a potent inhibitor of the JAK family with IC_{50} values of 2.8 nM, 2.6 nM, 13 nM, and 58 nM for JAK1/2/3 and Tyk2, respectively [114]. A summary of the JAK family of nonreceptor protein-tyrosine kinases and downstream signaling by the STAT proteins is provided in Section 4.11. Noji et al. solved the X-ray crystal structure of delgocitinib bound to JAK3 [115]. They found that the drug hydrogen bonded to the backbone C═O of E903 (the first hinge residue), the backbone N–H of L905 (the third hinge residue), and the C═O of G831 within the G-rich loop (Fig. 5D). The drug interacts hydrophobically with two shell residues (Sh1/2), three catalytic spine residues (CS6/7/8), and the Klifs-3 residue (Table 5). The medicinal also interacts hydrophobically with G829, K830, G831, and G834 of the G-rich loop, S835 of the β2-strand, K855 of the β3-strand, M902 (the gatekeeper residue), E903, L905, C909 of the hinge-linker segment, R953, N954 of the catalytic loop, A966 (the x of xDFG), and DFG-D967 of the activation segment. The drug is found in the front pocket and FP-I/II. Modi and Dunbrack classify the enzyme in this complex as the inactive ABAminus structure [33]. We accordingly label the complex as a type I½ B inhibitor because the drug does not extend into the back cleft of an inactive DFG-D_{in} enzyme [44]. The medicine is listed in 14 clinical trials of which nine have been completed (Table 6). See Refs. [113,115, 116] for summaries of the efficacy of delgocitinib in clinical trials.

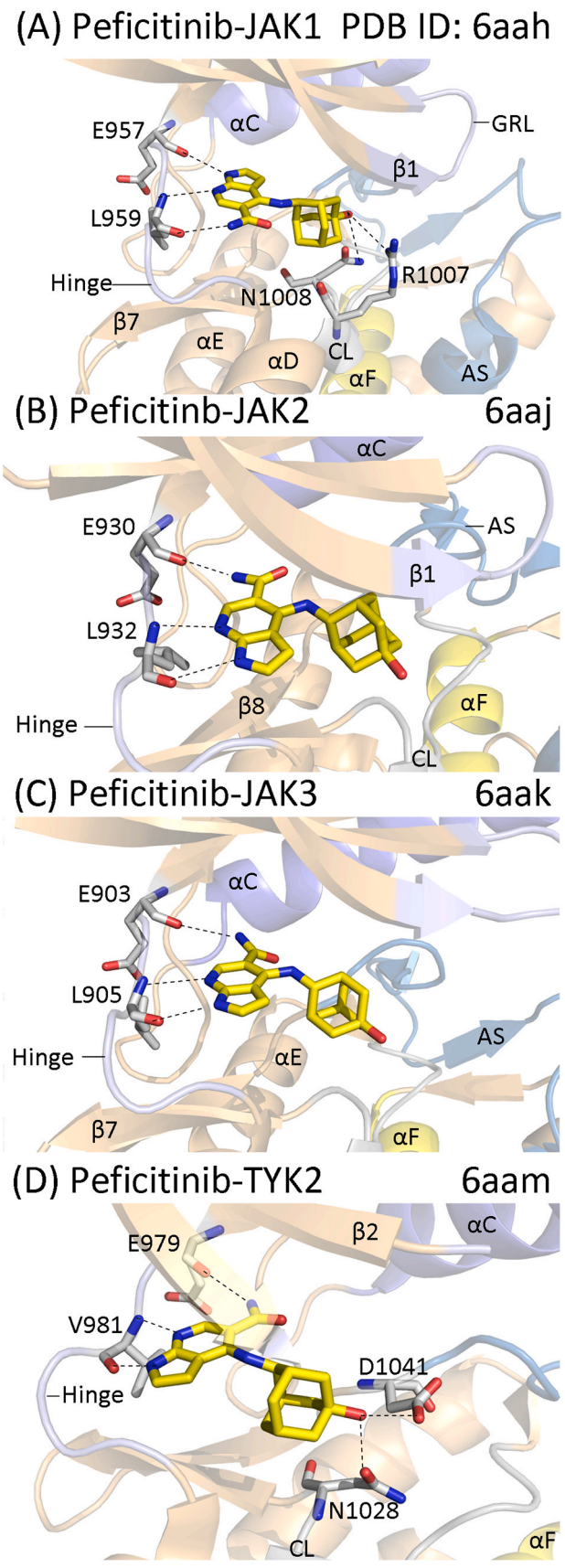

Fig. 6. Peficitinib-enzyme complexes. AS, activation segment; CL, catalytic loop; GRL, glycine-rich loop. Dashed lines represent polar bonds.

4.15. Pyrotinib, an EGFR inhibitor

Pyrotinib is an ethoxyquinoline derivative (Fig. 4O) that was approved in China (2020) in combination with capecitabine for the treatment of HER2-positive advanced or metastatic breast cancer in patients previously treated with anthracycline or taxane chemotherapy [117,118]. The IC_{50} value of this agent for EGFR is 5.6 nM and that for ErbB2 (HER2) is 8.1 nM [117]. A summary of the properties of the epidermal growth factor receptor family is provided in Section 4.2. This medicinal is listed in 159 clinical trials of which 12 have been completed (Table 6). See Refs. [117–121] for summaries of the pharmacology of pyrotinib and clinical trials examining its effectiveness.

4.16. Orelabrutinib, a BTK antagonist

Orelabrutinib is a pyridine-3-carboxamide derivative (Fig. 4P) that was approved in China for the treatment of patients with relapsed/refractory chronic lymphocytic leukemia, small lymphocytic lymphoma, and relapsed/refractory mantle cell lymphoma in 2020 [122]. The IC_{50} value for its BTK target is 1.6 nM [122]. The role of BTK in the functioning of B cells is outlined in Section 4.13. This agent is listed in 36 clinical trials of which two have been completed (Table 6). Although we lack the X-ray crystal structure of orelabrutinib with its cognate enzyme, the drug is a targeted covalent inhibitor (TCI) so that we can classify it as a type VI inhibitor [44]. See Refs. [122,123] for a summary of the pharmacological properties and clinical trials addressing the clinical efficacy of orelabrutinib.

4.17. Peficitinib, a JAK family blocker

Peficitinib is a pyrrolo[2,3-*b*]pyridine-5-carboxamide derivative (Fig. 4Q) that is approved in Japan for the treatment of rheumatoid arthritis (including the prevention of structural joint damage) in patients who had an inadequate response to conventional therapies [124]. The IC_{50} values for its JAK family enzymes were 3.9 nM, 5.0 nM, 0.71 nM, and 4.8 nM against JAK1, JAK2, JAK3, and Tyk2, respectively [125]. It thus is a potent antagonistic with some selectivity for JAK3. Hamaguchi et al. determined the X-ray crystal structure of peficitinib with each of these enzymes [125]. They found that the nitrogen atoms of the pyrrolo-pyridine formed hydrogen bonds with the first and third JAK1 hinge residues (E957 and L959) and the hydroxyl group hydrogen-bonded with the side chains of R1007 and N1008 of the catalytic loop (Fig. 6A). The medicinal makes hydrophobic contact with two shell residues (Sh1/2), three catalytic spine residues (CS6/7/8), and the Klifs-3 residue (Table 5). The drug also interacts hydrophobically with G882 of the G-rich loop, the gatekeeper residue (M956), F958, L959, G962, and S963 of the hinge-linker segment, R1007 of the catalytic loop, G1020 (the x of xDFG), and DFG-D1021 of the activation segment. The drug occurs in the front pocket and FP-I (Klifs.net). The enzyme in this complex has an inactive ABAminus conformation with DFG-D_{in} [33] and we classify it as a type I½ B inhibitor [44].

Hamaguchi et al. found that peficitinib makes one hydrogen bond with the backbone C═O of E930 (the first hinge residue) and two hydrogen bonds with the backbone C═O and N–H groups of L932 (the third hinge residue) of JAK2 (Fig. 6B) [125]. As in the case of JAK1, the drug makes hydrophobic contact with the JAK2 Sh1 and Sh2 shell residues, CS6/7/8, and the Klifs-3 residue (Table 5). The drug also interacts hydrophobically with G856 of the G-rich loop, M929 (the gatekeeper residue), Y931, L932, G935, and S936 of the hinge-linker segment, and DFG-D 994 of the activation segment. The drug occupies the front pocket and FP-I. The enzyme in this complex has the BLAminus conformation, which corresponds to the active conformation in the Modi and Dunbrack scheme [33]. We therefore classify peficitinib as a type I inhibitor of JAK2 [44].

Hamaguchi et al. reported that peficitinib forms a hydrogen bond with the backbone C═O of E903 (the first hinge residue) and forms two

hydrogen bonds with the backbone C═O and N–H groups of L905 (the third hinge residue) of JAK3 (Fig. 6C) [125]. As in the case of JAK1/2, the drug makes hydrophobic contact with the JAK3 Sh1 and Sh2 shell residues, CS6/7/8, and the Klifs-3 residue (Table 5). The drug also interacts hydrophobically with G829 of the G-rich loop, M902 (the gatekeeper residue), Y904 and G908 of the hinge-linker segment, A966 (the x of xDFG), and DFG-D 967 of the activation segment. The drug occupies the front pocket and FP-I. The enzyme in the complex has the BLAminus conformation, which corresponds to the active conformation in the Modi and Dunbrack scheme [33]. We therefore classify peficitinib as a type I inhibitor of JAK3 [44].

Hamaguchi et al. found that peficitinib makes one hydrogen bond with the backbone C═O of E979 (the first hinge residue) and two hydrogen bonds with the backbone C═O and N–H groups of V981 (the third hinge residue) of Tyk2 [125]. The hydroxyl group of the drug hydrogen bonds with the R-groups of N1028 of the catalytic loop and DFG-D1041 of the activation segment (Fig. 6D). As in the case of JAK1/2/3, the drug makes hydrophobic contact with the Tyk2 Sh1 and Sh2 shell residues, CS6/7/8, and the Klifs-3 residue (Table 5). The drug also interacts hydrophobically with G904 of the G-rich loop, M978 (the gatekeeper residue), Y980, V981, G984, and S985 of the hinge-linker segment, and DFG-D1041of the activation segment. The drug occupies the front pocket and FP-I (Klifs.net). The enzyme in the complex has the BLAminus conformation, which corresponds to the active conformation in the scheme of Modi and Dunbrack [33]. We therefore classify peficitinib as a type I inhibitor of Tyk2 [44]. Note that peficitinib flips as we go from JAK1 to JAK2/3 and Tyk2 (Fig. 6). The efficacy of peficitinib is or has been examined in 34 clinical trials of which 33 have been completed. See Refs. [124,126] for a synopsis of information obtained from clinical trials involving peficitinib.

4.18. Surufatinib, a VEGFR inhibitor

Surufatinib (sulfatinib) is an indole-pyrimidine derivative (Fig. 4R) that was approved in China for the treatment of late-stage, well-differentiated, extrapancreatic neuroendocrine tumors in 2021 [127]. Surufatinib (HMPL-012, previously known as sulfatinib) is an oral, small-molecule receptor protein-tyrosine kinase inhibitor that potently inhibits VEGFR1 (IC_{50} of 2 nM), VEGFR2 (IC_{50} of 24 nM), and VEGFR3 (IC_{50} of 1 nM) [128]. The drug is also a potent inhibitor of FGFR1 (IC_{50} value of 15 nM) and CSF-1R (IC_{50} of 4 nM). This unique combination of molecular activities inhibits tumor angiogenesis, regulates tumor-immune evasion, and may decrease tumor resistance. See Section 4.4 for a summary of the VEGFR protein-tyrosine kinase family and its ligands, Ref. [129] for a review of the FGFR1/2/3/4 protein-tyrosine kinase family and their ligands, and Ref. [130] for a summary of the CSF1R protein-tyrosine kinase and its ligands. The efficacy of surufatinib is or has been examined in 66 clinical trials of which 15 have been completed. See Refs. [127,128,131,132] for a summary of the information derived from clinical trials involving surufatinib.

4.19. Savolitinib, a MET receptor antagonist

Savolitinib is an imidazo[1,2-*a*]pyridine derivative (Fig. 4S) that was approved in China in 2021 for the treatment of metastatic NSCLC with *MET* exon 14-skipping alterations in patients who have progressed after or who are unable to tolerate platinum-based chemotherapy [133]. The *MET* gene encodes the hepatocyte growth factor receptor, a receptor protein-tyrosine kinase, that responds to the hepatocyte growth factor. For a discussion of the properties of the hepatocyte growth factor receptor, see Ref. [134]. This compound is a potent inhibitor of this receptor with an IC_{50} value of 4 nM [135]. The effectiveness of savolitinib has been examined in 41 clinical trials of which 15 have been completed (Table 6). For a discussion of the clinical trials that led to the approval of this drug, see Refs. [133,134,136,137].

4.20. Lazertinib, an EGFR blocker

Lazertinib is a phenylpyrazole-pyrimidine derivative (Fig. 4T) that is an orally bioavailable, third-generation, epidermal growth factor receptor (EGFR) protein-tyrosine kinase inhibitor that was approved in South Korea in 2021 for the treatment of patients with *EGFR T790M* mutation-positive locally advanced or metastatic NSCLC who have previously received EGFR protein kinase inhibitor therapy [138]. Lazertinib is a brain penetrant, irreversible antagonist that inhibits the *T790M* gatekeeper mutant and the activating *Ex19del* and *L858R EGFR* mutants, while sparing wildtype EGFR. See Section 4.2 for a summary of the properties and ligands of the EGFR family. The IC_{50} value of lazertinib for the EGFR T790M mutant is on the order of 2 nM. The efficacy of this compound has been studied in 33 clinical trials of which eight have been completed (Table 6). We lack the X-ray structure of this compound bound to its cognate enzyme, but we can classify it as a type VI inhibitor because it forms a covalent bond with its target [44]. See Refs. [138,139] for a summary of clinical trials that led to its approval.

4.21. Furmonertinib, an EGFR inhibitor

Furmonertinib (alflutinib) is an indole-pyrimidine derivative (Fig. 4U) that is approval in China (2021) for the treatment of patients with locally advanced or metastatic NSCLC with a confirmed *EGFR T790M* mutation whose disease has progressed during or after EGFR protein-tyrosine kinase inhibitor therapy [140]. See Section 4.2 for a summary of the physiological properties of the EGFR family and its ligands. The IC_{50} value of furmonertinib, which is an orally bioavailable inhibitor, for EGFR is on the order of 10 nM. The efficacy of this medicine has been studied in 32 clinical trials of which two have been completed. See Refs. [140,141] for a synopsis of the clinical trials that led to its approval. Although we lack the X-ray crystal structure of this compound bound to the EGFR T790M mutant protein, it can be classified as a type VI inhibitor based upon its ability to form a covalent bond with its enzyme target [44].

5. Physicochemical properties of orally bioavailable drugs

5.1. Lipinski's rule of five (Ro5)

Medicinal chemists and pharmacologists have examined the physicochemical properties of drugs that are orally effective. Lipinski's rule of five (Ro5) is a computational technique that is used to estimate drug solubility, drug membrane permeability, and pharmacological effectiveness in the drug-discovery setting [142]. This procedure is a rule of thumb that determines whether a compound with specific pharmacological activities has physical properties suggesting that it would be orally effective. The Lipinski rules are based on data showing that most orally effective compounds are relatively small and moderately lipophilic substances. Ro5 conformity is used during drug development as (i) effective hits discovered during high throughput screening and (ii) lead compounds are systematically optimized to improve their potency while maintaining selectivity and specificity.

The Ro5 criteria indicate that less than ideal oral bioavailability is more likely to occur when (i) the atom-based calculated Log P (ALogP) is above 5, when (ii) there are more than 5 hydrogen-bond donors, when (iii) there are more than 5×2 or 10 hydrogen-bond acceptors, and when (iv) the molecular weight exceeds 5×100 or 500 [142]. The partition coefficient (P) is the ratio of the solubility of the un-ionized drug in the organic phase divided by its solubility in the aqueous phase of water-saturated *n*-octanol. The P value reflects the hydrophobicity of a compound; the greater the P value, the greater the hydrophobicity. The number of hydrogen-bond donors represents the sum of NH and OH groups. The number of hydrogen-bond acceptors is more complicated to evaluate; these are the number of uncharged heteroatoms with the exception of halogens, heteroaromatic oxygen and sulfur

Table 7
Properties of small molecule protein kinase inhibitors approved outside of the United States[a].

Drug	PubMED CID	Formula	MW (Da)	HD[b]	HA[c]	ALogP[d]	$LogD_{7.4}$[d]	PSA (Å)^2[e]	Complexity[f]	Fsp^3[g]
Fasudil	3547	$C_{14}H_{17}N_3O_2S$	291.4	1	4	1.22	-0.40	70.7	421	0.36
Icotinib	22024915	$C_{22}H_{21}N_3O_4$	391.4	1	7	3.16	3.03	74.7	553	0.27
Ripasudil	9863672	$C_{15}H_{18}FN_3O_2$	323.4	1	4	1.75	0.02	70.7	482	0.40
Apatinib	11315474	$C_{24}H_{23}N_5O$	397.5	2	5	4.68	4.29	90.7	608	0.25
Radotinib	16063245	$C_{27}H_{21}F_3N_8O$	530.5	2	8	5.75	4.52	110.5	818	0.11
Olmutinib	54758501	$C_{26}H_{26}N_5O_2S$	486.6	2	8	5.10	4.81	82.6	712	0.19
Simotinib	16735117	$C_{25}H_{26}ClFN_4O_4$	500.9	1	8	4.39	4.47	78	742	0.40
Catequentinib	25017411	$C_{23}H_{22}FN_3O_3$	407.4	2	6	4.83	1.38	82.4	606	0.26
Fruquintinib	44480399	$C_{21}H_{19}N_3O_5$	393.4	1	7	3.85	2.64	95.7	570	0.19
Flumatinib	46848036	$C_{29}H_{29}F_3N_8O$	562.6	2	11	5.00	3.26	99.2	841	0.28
Filgotinib	49831257	$C_{21}H_{23}N_5O_3$	425.5	1	7	1.98	2.03	105	715	0.38
Almonertinib	121280087	$C_{30}H_{35}N_7O_2$	525.7	2	8	5.31	3.47	87.6	823	0.30
Tirabrutinib	54755438	$C_{25}H_{22}N_nO$	454.5	1	6	2.75	3.27	105	825	0.20
Delgocitinib	50914062	$C_{16}H_{18}N_6O$	310.4	1	5	1.30	0.60	88.9	544	0.50
Pyrotinib	51039030	$C_{32}H_{31}ClN_6O_3$	583.1	2	8	5.63	?	112.4	960	0.25
Orelabrutinib	91667513	$C_{26}H_{25}N_3O_3$	427.5	1	4	4.53	3.74	85.5	647	0.19
Peficitinib	57928403	$C_{18}H_{22}N_4O_2$	326.4	4	4	2.01	1.05	104	525	0.50
Surufatinib	52920501	$C_{24}H_{28}N_6O_3S$	480.6	3	7	3.78	2.82	121	733	0.25
Savolitinib	68289010	$C_{17}H_{15}N_9$	345.4	0	9	1.88	1.03	91.6	505	0.18
Lazertinib	121269225	$C_{30}H_{34}N_8O_3$	554.6	2	9	4.10	3.56	110	837	0.27
Furmonertinib	118861389	$C_{28}H_{31}F_3N_8O_2$	586.6	2	11	4.84	4.05	100	865	0.29

[a] Data from https://www.ppu.mrc.ac.uk/list-clinically-approved-kinase-inhibitors.
[b] HD, No. of hydrogen bond donors.
[c] HA, No. of hydrogen bond acceptors.
[d] Values for atom-based log of the partition coefficient (ALogP) and $LogD_{7.4}$ from https://www.ebi.ac.uk/chembl/.
[e] PSA, polar surface area.
[f] Complexity values obtained from https://pubchem.ncbi.nlm.nih.gov/.
[g] Fsp^3, Fraction of sp^3 carbon atoms or no. of sp^3 carbon atoms ÷ total no. of carbon atoms.

atoms, pyrrole nitrogen atoms, and higher oxidation states of phosphorus, sulfur, and nitrogen, but it includes the oxygen atoms bonded to them. In the original paper [142], the number of hydrogen bond acceptors equaled the sum of nitrogen and oxygen atoms. The Ro5 benchmarks were based on the physicochemical properties of 2245 reference drugs that had reached phase II clinical trials or higher and the final values were at the 90th percentile for the distribution of the four components in the original Ro5 criteria [142]. If any two of the four conditions were violated, the molecule was deemed less likely to result in an orally bioavailable drug. Actively transported molecules and natural products were excluded from this analysis.

One-third of the 21 internationally approved drugs considered in this article are not Ro5 compliant. Pyrotinib (583.1 Da), lazertinib (554.6 Da), and simotinib (500.9 Da) have molecular weights exceeding 500 (Table 7). Radotinib, flumatinib, and almonertinib have molecular weights and AlogP values greater than 500 Da and 5.0, respectively. Furmonertinib has two Ro5 violations with a molecular weight of 586.6 and 11 hydrogen bond acceptors. The single greatest Ro5 violation of small molecule protein kinase inhibitors approved by the FDA is also the molecular weight (22 of 75 drugs) and the next greatest violation is associated with the AlogP value (20 of 75 drugs) [143]. Medicinals with Ro5 noncompliance are labeled bRo5 (beyond the rule of five) compounds.

5.2. The importance of lipophilicity and ligand efficiency

5.2.1. Lipophilic efficiency, LipE

Both before and after the advent of Lipinski's Ro5 in 2001 [142], other studies of the physicochemical properties of orally effective medicinal were published [144–151]. For instance, LipE (lipophilic efficiency) is a parameter that is used in drug discovery and development that combines potency and lipophilic-driven binding as a strategy to increase binding affinity. The ensuing formulas are used to calculate lipophilic efficiency:

$$\text{LipE} = \text{p}K_\text{i} - \text{ALogP};\ \text{LipE} = \text{pIC}_{50} - \text{ALogP}$$

Similar to the practice of expressing the molar hydrogen ion concentration as pH, the operator p denotes the negative of the Log_{10} of the K_i or IC_{50}. ALogP is the atom-based computed Log_{10} of the partition coefficient; this parameter reflects the ratio of the drug solubility in the organic phase divided by its solubility in the aqueous phase of immiscible *n*-octanol/water. The second term of the equation (– ALogP or minus ALogP) denotes the lipophilicity of a compound and the value is calculated using an algorithm reflecting the characteristics of thousands of reference organic chemicals. The greater the solubility of a substance in the organic phase as compared with the aqueous phase of a *n*-octanol/water mixture, the greater is its lipophilicity. Leeson and Springthorpe asserted that drug lipophilicity, as assessed by its – ALogP value, is one of the more important parameters that should be evaluated during the drug discovery process [145]. Their use of ALogP was based upon calculations performed before the evaluation of the distribution coefficient (D) became more common. The distribution coefficient ($LogD_{7.4}$) represents the ratio of the solubility of the ionized and un-ionized drug in the organic phase over the aqueous phase of immiscible *n*-octanol/water at a specified pH of the aqueous phase, which is usually 7.4. As a practical matter, either ALogP or $LogD_{7.4}$ can be used to evaluate several agents in the same study. Note that a highly lipophilic substance with a large negative – ALogP value decreases the lipophilic efficiency. The goal in drug development is to maximize lipophilic efficiency – maximize potency and minimize lipophilicity.

The ALogP of various drugs can be calculated in a matter of seconds. Because the experimental determination of LogP is demanding, such measurements are performed in only select cases. Hopkins et al. reported that appropriate values for LogP are less than ~ 3 and those of lipophilic efficiency are greater than ~ 5 [147]. Johnson et al. indicated that having a $LogD_{7.4}$ in the range of 1 – 3 provides the best chance of achieving the overlap of low renal clearance, low hepatic oxidative clearance, high solubility, and high passive permeability [152]. The average value for $LogD_{7.4}$ for the 21 internationally approved drugs (Table 7) was 2.71. Only 6 of the internationally approved protein kinase antagonists have an $LogD_{7.4}$ in the 1–3 range and 12 have a value in the 1–4 range. The average value of lipophilic efficiency (LipE) for the 21 internationally approved small molecule protein kinase blockers listed in this article is 4.50 with a range from 1.72 (radotinib) to 7.25

Table 8
Properties of small molecule protein kinases inhibitors approved outside of the United States.

Drug	Target	IC_{50}, nM[b]	pK_i	N[c]	ALogP	LE[d]	LipE[e]	nRotB[f]	nRng[g]	nAr[hh]	nBnz[i]	QED[j]
Fasudil	ROCK1/2	530	6.28	20	1.22	0.443	5.06	2	3	2	0	0.90
Icotinib	EGFR	5	8.30	29	3.16	0.404	5.14	3	4	3	1	0.67
Ripasudil	ROCK1/2	51	7.29	22	1.75	0.467	5.54	2	3	2	0	0.91
Apatinib	VEGFR2	1	9.00	30	4.68	0.423	4.32	6	4	3	1	0.63
Radotinib	Abl	34	7.47	39	5.75	0.270	1.72	6	5	5	2	0.29
Olmutinib	EGFR	10	8.00	35	5.1	0.322	2.90	7	5	4	2	0.35
Simotinib	EGFR	19.9	7.70	35	4.39	0.310	3.31	7	6	3	1	0.51
Catequentinib	VEGFR2	0.2	9.70	30	4.83	0.456	4.88	6	5	4	0	0.48
Fruquintinib	VEGFR2	35	7.46	29	3.85	0.363	3.61	5	4	4	0	0.55
Flumatinib	BCR-Abl	1.2	8.92	41	5	0.307	3.92	7	5	4	1	0.32
Filgotinib	JAK1	10	8.00	30	1.98	0.376	6.02	5	5	3	1	0.67
Almonertinib	EGFR	3.4	8.47	39	5.31	0.306	3.16	11	5	4	1	0.26
Tirabrutinib	BTK	6.8	8.17	34	2.75	0.339	5.42	4	5	3	2	0.48
Delgocitinib	JAK1	2.8	8.55	23	1.3	0.524	7.25	2	4	2	0	0.90
Pyrotinib	EGFR	5.6	8.25	42	5.63	0.277	2.62	10	5	4	1	?
Orelabrutinib	BTK	1.6	8.80	32	4.53	0.388	4.27	6	4	3	2	0.59
Peficitinib	JAK3	0.71	9.15	24	2.01	0.538	7.14	3	5	2	0	0.69
Surufatinib	VEGFR2	24	7.62	34	3.78	0.316	3.84	10	4	4	1	0.32
Savolitinib	MET	4	8.40	26	1.88	0.456	6.52	3	5	5	0	0.50
Lazertinib	EGFR	2	8.70	41	4.1	0.299	4.60	10	5	4	1	0.28
Furmonertinib	EGFR	10	8.00	41	4.84	0.275	3.16	11	4	4	0	0.25

[a]Drugs listed in https://www.ppu.mrc.ac.uk/list-clinically-approved-kinase-inhibitors.
[b] Representative values obtained from www.ebi.ac.ug/chembl/ and from klifs.net.
[c] N, Number of heavy (nonhydrogen) atoms.
[d] LE (ligand efficiency) = – 2.303 RT Log_{10} K_i/N where N is the number of heavy (non-hydrogen) atoms in the drug.
[e] LipE (lipophilic efficiency) = pIC_{50} – AlogP.
[f] nRotB, no. of rotatable bonds.
[g] nRng, no. of rings.
[h] nAr, no. of aromatic rings.
[i] nBnz, no. of benzene moieties.
[j] QED, summed, weighted desirability (scores using MW + ALogP + HBD + HBA + PSA + nRotB + nAr) obtained from https://www.ebi.ac.uk/chembl/; see Ref. [151] for a full explanation.

(delgocitinib) with a standard deviation of 1.49 (Table 8).

5.2.2. *Ligand efficiency, LE*

The ligand efficiency (LE) relates the potency, or binding affinity, to the number of heavy (nonhydrogen) atoms of a drug. The following formula is used to compute this parameter:

$$LE = \Delta G^{\circ\prime}/N = -RT \ln K_{eq}/N = -2{\cdot}303RT \text{ Log } K_{eq}/N$$

$\Delta G^{\circ\prime}$ is the standard free energy change of a drug binding to its target at neutral pH, R denotes the universal gas constant or energy-temperature coefficient (1.98×10^{-3} kcal/degree-mol), T is the temperature in degrees Kelvin, K_{eq} represents the value of the equilibrium constant, and N is the number of heavy atoms in the drug. The K_i or IC_{50} values are substitutes for the equilibrium constant. At a physiological temperature of 37 °C (310 K), this equation becomes – (2.303 × (1.98×10^{-3}/K) × 310 K Log K_{eq})/N or – 1.41 Log K_{eq}/N [147]. At a temperature of 300 K (about room temperature), the multiplication factor is – 1.37 [151]. Ligand efficiency represents the affinity based on the average binding energy per heavy atom. Furthermore, ligand efficiency is useful in fragment-based drug discovery and it aids in the selection of promising derivatives of lead compounds for further development [148].

Ligand efficiency represents the binding affinity per heavy atom of the ligand or drug of interest. The value of N is a substitute for the molecular weight or size of the drug. The equation used to compute ligand efficiency indicates that its value is directly proportional to – Log K_{eq} (minus Log K_{eq}, a positive number) or the binding affinity and is inversely proportional to the number of heavy atoms. Hopkins et al. reported that optimal values for ligand efficiency (LE) should be greater than 0.3 kcal per mol of heavy atom [144,147]. Ligand efficiency values for the internationally approved small molecule protein kinase blockers (Table 1) based upon representative K_i or IC_{50} values are included in Table 8. The average value for ligand efficiency for the internationally approved protein kinase inhibitors was 0.374 with a range from 0.270 (radotinib) to 0.538 (peficitinib) with a standard deviation of 0.082. The values for ligand efficiency (LE) and lipophilic efficiency (LipE) listed in Table 8 are based on data acquired under different conditions. Accordingly, these values cannot be used to make a direct comparison of these agents because different methods were used to obtain the data. These findings were mined from various drug discovery projects and indicate typical values. The values for the 21 internationally approved drugs (Table 1) are very close to the values for the 75 FDA-approved drugs [143].

5.2.3. *Additional chemical descriptors of orally bioavailable drugs*

To characterize physicochemical parameters associated with oral bioavailability, not unexpectedly, the Ro5 has generated many variations and corollaries. For instance, Veber et al. reported that the number of rotatable bonds and the topological polar surface area (PSA) differentiates between orally active and inactive agents for a large series of compounds in rats [149]. They found that the optimal number of rotatable bonds is 10 or fewer. This property regulates passive membrane permeation and reflects molecular flexibility or degrees of freedom. Moreover, degrees of freedom are related to the entropy change associated with ligand binding. With the exceptions of two drugs with 11 rotatable bonds, the remaining 19 drugs have 10 or fewer of these bonds. The average value is 6.0 and the number of rotatable bonds ranges from 2 (ripasudil, delgocitinib) to 11 (filgotinib, furmonertinib) with a standard deviation of 3.0. Furthermore, Veber et al. found in general that drugs with a polar surface area less than or equal to 140 $Å^2$ are orally bioavailable [149]. This property represents the sum of the surface over all polar atoms, primarily nitrogen and oxygen, but it also includes any connected hydrogen atoms. The average value for the surface area is 93.6 $Å^2$ with a range from 70.7 (fasudil) to 121 (surufatinib) with a standard deviation of 14.4 (Table 7). Additionally, Oprea reported that the number of ring structures (both aromatic and

nonaromatic) in most orally bioavailable drugs is three or greater [150]. All of the internationally approved small molecule protein kinase antagonists have three or more rings with an average value of 4.52, a range from three to six, with a standard deviation of 0.75. Except for ripasudil (an eye drop) and delgocitinib (a topical cream), all of the internationally approved drugs covered in this article are orally effective.

Ritchie and Macdonald investigated aromaticity as a factor in the drug discovery process [153]. Aromaticity denotes cyclically conjugated chemicals with significantly greater stability than is found in localized Kekulé structures because of electron delocalization. These investigators classified bicyclic and tricyclic structures as those containing two and three aromatic rings, respectively. The aromatic ring count comprises structures containing carbon and heteroatom components. These authors found that increasing the number of carboaromatic rings (benzene moieties) has a deleterious effect on drug efficacy by decreasing water solubility, increasing attachment to serum albumin, and blocking cytochrome P450. We find that the average number of aromatic rings in the 21 internationally approved protein kinase inhibitors was 3.43 and the mean number of benzene moieties was 0.81. All of these approved kinase inhibitors have at least two aromatic rings; moreover, radotinib and savolitinib had the largest number of aromatic rings with five. Seven of the drugs lacked benzene moieties and the number of drugs possessing one or two benzenes was about evenly distributed among the remainder (Table 8).

The molecular complexity of a drug is a reflection of the elements it contains, its structural features, and its symmetry. This property is calculated using the Bertz/Hendrickson/Ihlenfelt algorithm [154,155]. The calculation depends upon the identity and number of the constituent atoms, the bonding arrangement, and the nature of the chemical bonds (single, double, triple, aromatic). Molecular complexity values range from 0 for simple ions to several thousand for intricate natural products. Ionic lithium, with a complexity of 0 and a molecular weight of 3, is used in the treatment of manic-depressive disorders and is dispensed as lithium carbonate (Li_2CO_3). In general, larger compounds have a greater molecular complexity value than smaller ones. In comparison, chemicals containing fewer elements and those that are highly symmetrical have a smaller molecular complexity value. The molecular complexity values for the drugs in this article were acquired from PubChem (https://pubchem.ncbi.nlm.nih.gov/). For the 21 internationally approved small molecule protein kinase antagonists (Table 1), the mean complexity value was 682 with a range from 421 (fasudil) to 960 (pyrotinib) with a standard deviation of 150 (Table 7). There are no optimal or recommended molecular complexity values for orally efficacious drugs; however, this property may be of use in predicting the ease or difficulty of drug synthesis, an important consideration in the commercial production of therapeutic entities.

Lovering et al. examined the fraction of sp^3 carbon atoms (Fsp^3) and the number of chiral carbon atoms as additional components of molecular complexity [156]. Fsp^3 is the number of sp^3 carbon atoms in an agent divided by the total number of carbon atoms. A larger value corresponds to (i) an increase in saturation of the chemical and (ii) a decrease in the number of unsaturated linkages including double and triple bonds and aromatic rings. Increased saturation allows for the synthesis of architecturally more complex molecules and results in the exploration of a more diverse chemical space without substantially increasing the molecular weight. These workers also suggest that increasing saturation will allow for the out-of-plane substituents to increase receptor-ligand complementarity and increase solubility. The mean Fsp^3 was 0.29 with a range of 0.11 (radotinib) to 0.50 (delgocitinib) with a standard deviation of 0.11. Regarding chirality, delgocitinib, peficitinib and savolitinib possess two stereocenters, ripasudil and tirabrutinib have one stereocenter, and the remainder of the internationally approved drugs (Table 1) lack a stereocenter.

From the above data, we surmise that medicinal chemists have drawn from compounds outside of the traditional Ro5 space to target an expanding number of protein kinases. It has been argued that a too strict implementation of the Ro5 may have hampered the pharmaceutical industry from exploring opportunities involving novel, but more difficult, targets [15,157]. Additional properties such as the number of rotatable bonds and the polar surface area have been used to extend correlations with absorption, distribution, metabolism, excretion, and toxicity (ADMET) properties. There has been a recent interest on decreasing the use of hard-cutoff rule-based classifications of drug candidates along with the emergence of composites such as the quantitative estimate of drug-likeness (QED). The QED (Table 8) includes weighted parameters of molecular weight, number of hydrogen-bond donors and acceptors, AlogP, number of rotatable bonds, polar surface area, and number of aromatic rings. The values for QED range from 0 (all properties unfavorable) to 1 (all properties favorable); the larger the value, the greater the drug-likeness. The mean value of QED for the internationally approved kinase inhibitors was 0.44 with a minimum of 0.25 (furmonertinib) and a maximum of 0.69 (peficitinib). These values are comparable to those of FDA-approved small molecule kinase blockers [3,4,17–21].

Table 9
Principal FDA-approved and internationally approved protein kinase inhibitor drug targets[a].

Kinase family	Class of Kinase	US FDA approved	Non-FDA approved
EGFR/ErbB	RY	9	6
VEGFR	RY	8	4
JAK	NRY	8	3
BCR-Abl	NRY	6	2
ALK	RY	5	
FGFR	RY	5	
CDK4/6	S/T	4	
MEK1/2	Y/T	4	
BTK	NRY	4	3
B-Raf	S/T	3	
FKBP	S/T	3	
MET	RY	3	1
Flt3	RY	2	
RET	RY	2	
ROCK	S/T	2	2
TRKA	RY	2	
CSF1	RY	1	
Kit	RY	1	
PDGFR	RY	1	
SYK	RY	1	
TYK2	NRY	1	
Total		75	21

[a] NYR, nonreceptor protein-tyrosine kinase; RY, receptor protein-tyrosine kinase; S/T, protein-serine/threonine kinase; Y/T, Dual specificity protein kinase – tyrosine phosphorylation followed by threonine phosphorylation of target kinase activation segments.

6. Epilogue and perspective

Although significant progress has been made in the development of low molecular weight protein kinase inhibitors since the approval of fasudil in 1995 in Japan and especially since the FDA-approval of imatinib in 2001 in the United States [18], this line of work is still in its infancy. Most of the internationally and FDA approved kinase inhibitors are antineoplastic and others function as immunomodulators [12,158–160]. Because of the inherent genetic changes in cancer cells, resistance to protein kinase inhibitors is the rule rather than the exception. Such resistance stimulated the discovery of second, third, and later generation antagonists that block the same enzyme. Furthermore, acquired drug resistance is often the result of gatekeeper mutations in the initial protein kinase target [5]. A gatekeeper mutation in *EGFR* (*T790M*) is a relevant example and this is the third most common protein kinase mutation. Moreover, this change is responsible for about half of all acquired *EGFR* inhibitor resistance mutations.

Because 244 protein kinase genes map to cancer amplicons and disease loci [13], it is likely that (i) a substantial increase in the number

Table 10
Drug properties and descriptors[a].

Category	Properties and descriptions
Size	Molecular weight (MW) and heavy atom count (N)
Lipophilicity	Calculated octanol–water partition coefficients (ALogP and Log $D_{7.4}$).
Polarity	Polar surface area (PSA), hydrogen-bond donors (HD) and hydrogen-bond acceptors (HA)
Aromatic and aliphatic descriptors	Number of rings (nRng), number of aromatic rings (nAr), number of benzene rings (nBnz), fraction of carbon atoms that are sp^3 hypridized (Fsp3), number of stereocenters (nStereo)
Flexibility	Number of rotatable bonds (nRotB)
Potency	$-Log_{10}$ molar concentration IC_{50} or K_i as pIC_{50} or pK_i
Ligand efficiency metrics	Lipophilic ligand efficiency or LipE = pIC_{50} – AlogP or pIC_{50} – Log $D_{7.4;}$ Ligand efficiency or LE = –2.303 RT K_{eq} /N
Composite physicochemical descriptors	Quantitative estimate of drug-likeness or QED = summed, weighted desirability (scores using MW + ALogP + HD + HA + PSA + nRotB + nAr)

[a] Adapted from Ref. [151].

of drugs blocking understudied protein kinases will be developed and (ii) new drugs will be developed for the treatment of additional illnesses [161–163]. Adding new protein kinases to the pharmacologic armamentarium will require the elucidation of signaling networks and pathways in addition to the phosphatidylinositol 3-kinase-AKT, the Ras/RAF/MEK/ERK, and the JAK-STAT signaling modules and protein kinases leading to these pathways [14,95,96,104–109]. As the protein kinase antagonist discipline progresses, it is expected that protein kinase inhibitors with new scaffolds, pharmacophores, and chemotypes will be devised [164]. Although eight allosteric inhibitors of protein kinases have been approved by the FDA (asciminib, cobimetinib, deucravacitinib, everolimus, selumetinib, sirolimus, temsirolimus, and trametinib), perhaps none of the inhibitors considered in this article (Table 1) are allosteric in nature. Because we lack X-ray crystal structures of 16 of the drugs reviewed in this article, it is possible that one or more is an allosteric inhibitor. However, it is likely that additional allosteric antagonists will be developed worldwide that block (i) well known and (ii) understudied enzymes that are components of protein kinase signal transduction modules [165,166].

Of the 21 internationally approved drugs considered in this article, receptor protein-tyrosine kinases are the chief targets of 11 drugs, nonreceptor protein-tyrosine kinases are the main targets of eight drugs, and two drugs block protein-serine/threonine kinases. The ErbB, VEGFR, and JAK families are the leading targets of the FDA and internationally approved drugs (Table 9).

Pfizer began the process of high throughput screening (HTS) in 1986 using 96-well plates and assay volumes of 50–100 μL [167]. By 1992 HTS produced hits as starting materials for about 40% of the drug discovery portfolio. By 1999 ADMET HTS was fully integrated into the drug discovery cycle. It was about this time that Ro5 compliance was introduced in an effort to maximize the development of effective drugs and the minimize the attrition or failure of drug candidates that were identified by HTS. Gefitinib, erlotinib, sorafenib, dasatinib, and lapatinib are FDA-approved protein kinase antagonists that resulted from HTS hits. Prior to the advent of high throughput screening, drug discovery was based upon experiments performed in animals in vivo.

The commonly used drug properties and descriptors used by medicinal chemists and pharmacologists are listed in Table 10. bRo5 descriptors include the heavy atom count, $LogD_{7.4}$, polar surface area, number of rings (total, aromatic, carboaromatic), number of rotatable bonds, potency, and composite metrics such as quantitative estimate of drug likeness (QED). Low solubility, poor passive cell permeability, and issues related to metabolism are associated with increased molecular weight and lipophilicity. These drawbacks need to be overcome when working in the bRo5 space. Increased molecular complexity oftentimes improves solubility and reduces adventitious binding to off-targets. On the other hand, increased molecular complexity increases the difficulty of synthesis. The protein kinase inhibitor field is a relatively new one and eight of the 21 internationally approved drugs considered in this article and 30 of the 75 FDA-approved drugs have a least one Ro5 violation. As stated by Hartung et al. “Playing by the rules is thus not always advisable when pushing for success in drug discovery. Rather, successful drug hunters must follow a mindset of pushing the limits of what is possible. Now, 25 years after the publication of the Ro5, small-molecule drug discovery is looking at an exciting future of clinical impact that must not be restricted by the number 5” [168].

Declaration of Competing Interest

The author is unaware of any affiliations, memberships, or financial holdings that might be perceived as affecting the objectivity of this review.

Acknowledgments

I am grateful to Laura M. Roskoski for providing editorial and bibliographic assistance. I thank Jasper Martinsek and Josie Rudnicki for their help in preparing the figures and W.S. Sheppard and Pasha Brezina for their help in curating and collating the data. Dr. Albert J. Kooistra kindly provided Fig. 3. The colored figures in this paper were evaluated to ensure that their perception was accurately conveyed to colorblind readers [169].

References

[1] P. Cohen, Protein kinases – the major drug targets of the twenty-first century? Nat. Rev. Drug Discov. 1 (2002) 309–315, https://doi.org/10.1038/nrd773.
[2] R. Roskoski Jr., A historical overview of protein kinases and their targeted small molecule inhibitors, Pharmacol. Res 100 (2015) 1–23, https://doi.org/10.1016/j.phrs.2015.07.010.
[3] R. Roskoski Jr., Properties of FDA-approved small molecule protein kinase inhibitors: a 2023 update, Pharmacol. Res 187 (2023), 106552, https://doi.org/10.1016/j.phrs.2022.106552.
[4] R. Roskoski Jr., Futibatinib (Lytgobi) for cholangiocarcinoma, Trends Pharm. Sci. 44 (2023) 190–191, https://doi.org/10.1016/j.tips.2022.12.007.
[5] P. Cohen, D. Cross, P.A. Jänne, Kinase drug discovery 20 years after imatinib: progress and future directions, Nat. Rev. Drug Discov. 20 (2021) 551–569, https://doi.org/10.1038/s41573-021-00195-4.
[6] M.M. Attwood, D. Fabbro, A.V. Sokolov, S. Knapp, H.B. Schiöth, Trends in kinase drug discovery: targets, indications and inhibitor design, Nat. Rev. Drug Discov. 20 (2021) 798, https://doi.org/10.1038/s41573-021-00303-4.
[7] G.K. Kanev, C. de Graaf, I.J.P. de Esch, R. Leurs, T. Würdinger, B.A. Westerman, A.J. Kooistra, The landscape of atypical and eukaryotic protein kinases, Trends Pharm. Sci. 40 (2019) 818–832, https://doi.org/10.1016/j.tips.2019.09.002.
[8] M. Shibuya, T. Asano, Y. Sasaki, Effect of Fasudil HCl, a protein kinase inhibitor, on cerebral vasospasm, Acta Neurochir. Suppl. 77 (2001) 201–204, https://doi.org/10.1007/978-3-7091-6232-3_42.
[9] M. Shibuya, Y. Suzuki, M. Takayasu, T. Asano, T. Harada, I. Ikegaki, S. Satoh, H. Hidaka, The effects of an intracellular calcium antagonist HA 1077 on delayed cerebral vasospasm in dogs, Acta Neurochir. (Wien.) 90 (1988) 53–59, https://doi.org/10.1007/BF01541267.
[10] N. Ono-Saito, I. Niki, H. Hidaka, H-series protein kinase inhibitors and potential clinical applications, Pharm. Ther. 82 (1999) 123–131, https://doi.org/10.1016/s0163-7258(98)00070-9.
[11] F. Carles, S. Bourg, C. Meyer, P. Bonnet, PKIDB: a curated, annotated and updated database of protein kinase inhibitors in clinical trials, Molecules 23 (2018) pii: E908, https://doi.org/10.3390/molecules23040908.
[12] C.C. Ayala-Aguilera, T. Valero, Á. Lorente-Macías, D.J. Baillache, S. Croke, A. Unciti-Broceta, Small molecule kinase inhibitor drugs (1995-2021): medical indication, pharmacology, and synthesis, J. Med Chem. 65 (2022) 1047–1131, https://doi.org/10.1021/acs.jmedchem.1c00963.
[13] G. Manning, D.B. Whyte, R. Martinez, T. Hunter, S. Sudarsanam, The protein kinase complement of the human genome, Science 298 (2002) 1912–1934, https://doi.org/10.1126/science.1075762.
[14] R. Roskoski Jr., Properties of FDA-approved small molecule phosphatidylinositol 3-kinase inhibitors prescribed for the treatment of malignancies, Pharmacol. Res 168 (2021), 105579, https://doi.org/10.1016/j.phrs.2021.105579.
[15] B.C. Doak, B. Over, F. Giordanetto, J. Kihlberg, Oral druggable space beyond the rule of 5: insights from drugs and clinical candidates, Chem. Biol. 21 (2014) 1115–1142, https://doi.org/10.1016/j.chembiol.2014.08.013.
[16] R. Roskoski Jr., Orally effective FDA-approved protein kinase targeted covalent inhibitors (TCIs), Pharmacol. Res 165 (2021), 105422, https://doi.org/10.1016/j.phrs.2021.105422.

[17] R. Roskoski Jr., Deucravacitinib is an allosteric TYK2 protein kinase inhibitor FDA-approved for the treatment of psoriasis, Pharmacol. Res 189 (2023), 106642.
[18] R. Roskoski Jr., Properties of FDA-approved small molecule protein kinase inhibitors, Pharmacol. Res 144 (2019) 19–50, https://doi.org/10.1016/j.phrs.2019.03.006.
[19] R. Roskoski Jr., Properties of FDA-approved small molecule protein kinase inhibitors: a 2020 update, Pharmacol. Res 152 (2020), 104609, https://doi.org/10.1016/j.phrs.2019.104609.
[20] R. Roskoski Jr., Properties of FDA-approved small molecule protein kinase inhibitors: a 2021 update, Pharmacol. Res 165 (2021), 105463, https://doi.org/10.1016/j.phrs.2021.105463.
[21] R. Roskoski Jr., Properties of FDA-approved small molecule protein kinase inhibitors: A 2022 update, Pharmacol. Res 175 (2022), 106037, https://doi.org/10.1016/j.phrs.2021.106037.
[22] D.R. Knighton, J.H. Zheng, L.F. Ten Eyck, V.A. Ashford, N.H. Xuong, S.S. Taylor, J.M. Sowadski, Crystal structure of the catalytic subunit of cyclic adenosine monophosphate-dependent protein kinase, Science 253 (1991) 407–414, https://doi.org/10.1126/science.1862342.
[23] A.P. Kornev, S.S. Taylor, Dynamics-driven allostery in protein kinases, Trends Biochem Sci. 40 (2015) 628–647, https://doi.org/10.1016/j.tibs.2015.09.002.
[24] S.S. Taylor, J. Wu, J.G.H. Bruystens, J.C. Del Rio, T.W. Lu, A.P. Kornev, L.F. Ten Eyck, From structure to the dynamic regulation of a molecular switch: a journey over 3 decades, J. Biol. Chem. 296 (2021), 100746, https://doi.org/10.1016/j.jbc.2021.100746.
[25] R. Roskoski Jr., Cyclin-dependent protein serine/threonine kinase inhibitors as anticancer drugs, Pharmacol. Res 139 (2019) 471–488, https://doi.org/10.1016/j.phrs.2018.11.035.
[26] R. Roskoski Jr., Hydrophobic and polar interactions of FDA-approved small molecule protein kinase inhibitors with their target enzymes, Pharmacol. Res 169 (2021), 105660, https://doi.org/10.1016/j.phrs.2021.105660.
[27] S.K. Hanks, T. Hunter, Protein kinases 6. The eukaryotic protein kinase superfamily: kinase (catalytic) domain structure and classification, FASEB J. 9 (1995) 576–596.
[28] Madhusudan, E.A. Trafny, N.H. Xuong, J.A. Adams, L.F. Ten Eyck, S.S. Taylor, J. M. Sowadski, cAMP-dependent protein kinase: crystallographic insights into substrate recognition and phosphotransfer, Protein Sci. 3 (1994) 176–187, https://doi.org/10.1002/pro.5560030203.
[29] J. Zhou, J.A. Adams, Participation of ADP dissociation in the rate-determining step in cAMP-dependent protein kinase, Biochemistry 36 (1997) 15733–15738, https://doi.org/10.1021/bi971438n.
[30] P.A. Schwartz, B.W. Murray, Protein kinase biochemistry and drug discovery, Bioorg. Chem. 39 (2011) 192–210, https://doi.org/10.1016/j.bioorg.2011.07.004.
[31] A.P. Kornev, S.S. Taylor, Defining the conserved internal architecture of a protein kinase, Biochim Biophys. Acta 1804 (2010) 440–444, https://doi.org/10.1016/j.bbapap.2009.10.017.
[32] V. Modi, R.L. Dunbrack Jr., Defining a new nomenclature for the structures of active and inactive kinases, Proc. Natl. Acad. Sci. USA 116 (2019) 6818–6827, https://doi.org/10.1073/pnas.1814279116.
[33] V. Modi, R.L. Dunbrack, Kincore: a web resource for structural classification of protein kinases and their inhibitors, Nucleic Acids Res 50 (D1) (2022) D654–D664, https://doi.org/10.1093/nar/gkab920.
[34] A.P. Kornev, N.M. Haste, S.S. Taylor, L.F. Eyck, Surface comparison of active and inactive protein kinases identifies a conserved activation mechanism, Proc. Natl. Acad. Sci. USA 103 (2006) 17783–17788, https://doi.org/10.1073/pnas.0607656103.
[35] A.P. Kornev, S.S. Taylor, L.F. Ten Eyck, A helix scaffold for the assembly of active protein kinases, Proc. Natl. Acad. Sci. USA 105 (2008) 14377–14382, https://doi.org/10.1073/pnas.0807988105.
[36] H.S. Meharena, P. Chang, M.M. Keshwani, K. Oruganty, A.K. Nene, N. Kannan, S. S. Taylor, A.P. Kornev, Deciphering the structural basis of eukaryotic protein kinase regulation, PLoS Biol. 11 (2013), e1001690, https://doi.org/10.1371/journal.pbio.1001680.
[37] Y. Liu, K. Shah, F. Yang, L. Witucki, K.M. Shokat, A molecular gate which controls unnatural ATP analogue recognition by the tyrosine kinase v-Src, Bioorg. Med Chem. 6 (1998) 1219–1226, https://doi.org/10.1016/s0968-0896(98)00099-6.
[38] A.C. Dar, K.M. Shokat, The evolution of protein kinase inhibitors from antagonists to agonists of cellular signaling, Annu Rev. Biochem 80 (2011) 769–795, https://doi.org/10.1146/annurev-biochem-090308-173656.
[39] P.M. Ung, R. Rahman, A. Schlessinger, Redefining the protein kinase conformational space with machine learning, e2, Cell Chem. Biol. 25 (2018) 916–924, https://doi.org/10.1016/j.chembiol.2018.05.002.
[40] R. Hu, H. Xu, P. Jia, Z. Zhao, KinaseMD: kinase mutations and drug response database, Nucleic Acids Res 49 (D1) (2021) D552–D561, https://doi.org/10.1093/nar/gkaa945.
[41] F. Zuccotto, E. Ardini, E. Casale, M. Angiolini, Through the "gatekeeper door": exploiting the active kinase conformation, J. Med Chem. 53 (2010) 2691–2694, https://doi.org/10.1021/jm901443h.
[42] V. Lamba, I. Ghosh, New directions in targeting protein kinases: focusing upon true allosteric and bivalent inhibitors, Curr. Pharm. Des. 18 (2012) 2936–2945, https://doi.org/10.2174/138161212800672813.
[43] J.J. Liao, Molecular recognition of protein kinase binding pockets for design of potent and selective kinase inhibitors, J. Med Chem. 50 (2007) 409–424, https://doi.org/10.1021/jm0608107.
[44] R. Roskoski Jr., Classification of small molecule protein kinase inhibitors based upon the structures of their drug-enzyme complexes, Pharmacol. Res 103 (2016) 26–48, https://doi.org/10.1016/j.phrs.2015.10.021.
[45] O.P. van Linden, A.J. Kooistra, R. Leurs, I.J. de Esch, C. de Graaf, KLIFS: a knowledge-based structural database to navigate kinase-ligand interaction space, J. Med Chem. 57 (2014) 249–277, https://doi.org/10.1021/jm400378w.
[46] A.J. Kooistra, G.K. Kanev, O.P. van Linden, R. Leurs, I.J. de Esch, C. de Graaf, KLIFS: a structural kinase-ligand interaction database, Nucleic Acids Res 44 (D1) (2016) D365–D371, https://doi.org/10.1093/nar/gkv1082.
[47] G.K. Kanev, C. de Graaf, B.A. Westerman, I.J.P. de Esch, A.J. Kooistra, KLIFS: an overhaul after the first 5 years of supporting kinase research, Nucleic Acids Res (2020) gkaa895, https://doi.org/10.1093/nar/gkaa895.
[48] D. Bajusz, G.G. Ferenczy, G.M. Keserű, Structure-based virtual screening approaches in kinase-directed drug discovery, Curr. Top. Med Chem. 17 (2017) 2235–2259, https://doi.org/10.2174/1568026617666170224121313.
[49] M. Uehata, T. Ishizaki, H. Satoh, T. Ono, T. Kawahara, T. Morishita, H. Tamakawa, K. Yamagami, J. Inui, M. Maekawa, S. Narumiya, Calcium sensitization of smooth muscle mediated by a Rho-associated protein kinase in hypertension, Nature 389 (1997) 990–994, https://doi.org/10.1038/40187.
[50] S. Hartmann, A.J. Ridley, S. Lutz, The function of Rho-associated kinases ROCK1 and ROCK2 in the pathogenesis of cardiovascular disease, Front Pharm. 6 (2015) 276, https://doi.org/10.3389/fphar.2015.00276.
[51] R. Shahbazi, B. Baradaran, M. Khordadmehr, S. Safaei, A. Baghbanzadeh, F. Jigari, H. Ezzati, Targeting ROCK signaling in health, malignant and non-malignant diseases, Immunol. Lett. 219 (2020) 15–26, https://doi.org/10.1016/j.imlet.2019.12.012.
[52] Y. Feng, P.V. LoGrasso, O. Defert, R. Li, Rho kinase (ROCK) inhibitors and their therapeutic potential, J. Med Chem. 59 (2016) 2269–2300, https://doi.org/10.1021/acs.jmedchem.5b00683.
[53] Y. Xie, L. Yue, Y. Shi, X. Su, C. Gan, H. Liu, T. Xue, T. Ye, Application and study of ROCK inhibitors in pulmonary fibrosis: recent developments and future Perspectives, J. Med Chem. 66 (2023) 4342–4360, https://doi.org/10.1021/acs.jmedchem.2c01753.
[54] M. Jacobs, K. Hayakawa, L. Swenson, S. Bellon, M. Fleming, P. Taslimi, J. Doran, The structure of dimeric ROCK I reveals the mechanism for ligand selectivity, J. Biol. Chem. 281 (2006) 260–268, https://doi.org/10.1074/jbc.M508847200.
[55] Y.S. Guan, Q. He, M. Li, Icotinib: activity and clinical application in Chinese patients with lung cancer, Expert Opin. Pharm. 15 (2014) 717–728, https://doi.org/10.1517/14656566.2014.890183.
[56] R. Roskoski Jr., The ErbB/HER receptor protein-tyrosine kinases and cancer, Biochem Biophys. Res Commun. 319 (2004) 1–11, https://doi.org/10.1016/j.bbrc.2004.04.150.
[57] R. Roskoski Jr., The ErbB/HER family of protein-tyrosine kinases and cancer, Pharmacol. Res 79 (2014) 34–74, https://doi.org/10.1016/j.phrs.2013.11.002.
[58] R. Roskoski Jr., ErbB/HER protein-tyrosine kinases: Structure and small molecule inhibitors, Pharmacol. Res 87 (2014) 42–59, https://doi.org/10.1016/j.phrs.2014.06.001.
[59] R. Roskoski Jr., Small molecule inhibitors targeting the EGFR/ErbB family of protein-tyrosine kinases in human cancers, Pharmacol. Res 139 (2019) 395–411, https://doi.org/10.1016/j.phrs.2018.11.014.
[60] H. Sung, J. Ferlay, R.L. Siegel, M. Laversanne, I. Soerjomataram, A. Jemal, F. Bray, Global cancer statistics 2020: GLOBOCAN estimates of incidence and mortality worldwide for 36 cancers in 185 countries, CA Cancer J. Clin. 71 (2021) 209–249, https://doi.org/10.3322/caac.21660.
[61] F. Tan, X. Shen, D. Wang, G. Xie, X. Zhang, L. Ding, Y. Hu, W. He, Y. Wang, Y. Wang, Icotinib (BPI-2009H), a novel EGFR tyrosine kinase inhibitor, displays potent efficacy in preclinical studies, Lung Cancer 76 (2012) 177–182, https://doi.org/10.1016/j.lungcan.2011.10.023.
[62] Q. Zhao, J. Shentu, N. Xu, J. Zhou, G. Yang, Y. Yao, F. Tan, D. Liu, Y. Wang, J. Zhou, Phase I study of icotinib hydrochloride (BPI-2009H), an oral EGFR tyrosine kinase inhibitor, in patients with advanced NSCLC and other solid tumors, Lung Cancer 73 (2011) 195–202, https://doi.org/10.1016/j.lungcan.2010.11.007.
[63] Y. Shi, L. Zhang, X. Liu, C. Zhou, L. Zhang, S. Zhang, D. Wang, Q. Li, S. Qin, C. Hu, Y. Zhang, J. Chen, Y. Cheng, J. Feng, H. Zhang, Y. Song, Y.L. Wu, N. Xu, J. Zhou, R. Luo, C. Bai, Y. Jin, W. Liu, Z. Wei, F. Tan, Y. Wang, L. Ding, H. Dai, S. Jiao, J. Wang, L. Liang, W. Zhang, Y. Sun, Icotinib versus gefitinib in previously treated advanced non-small-cell lung cancer (ICOGEN): a randomised, double-blind phase 3 non-inferiority trial, Lancet Oncol. 14 (2013) 953–961, https://doi.org/10.1016/S1470-2045(13)70355-3.
[64] K.P. Garnock-Jones, Ripasudil: first global approval, Drugs 74 (2014) 2211–2215.
[65] Y. Kaneko, M. Ohta, T. Inoue, K. Mizuno, T. Isobe, S. Tanabe, H. Tanihara, Effects of K-115 (Ripasudil), a novel ROCK inhibitor, on trabecular meshwork and Schlemm's canal endothelial cells, Sci. Rep. 6 (2016), 19640, https://doi.org/10.1038/srep19640.
[66] H. Tanihara, T. Inoue, T. Yamamoto, Y. Kuwayama, H. Abe, H. Suganami, M. Araie, K-115 Clinical Study Group, Intra-ocular pressure-lowering effects of a Rho kinase inhibitor, ripasudil (K-115), over 24 h in primary open-angle glaucoma and ocular hypertension: a randomized, open-label, crossover study, Acta Ophthalmol. 93 (2015) e254–e260, https://doi.org/10.1111/aos.12599.
[67] H. Tanihara, T. Inoue, T. Yamamoto, Y. Kuwayama, H. Abe, M. Araie, K-115 Clinical Study Group, Phase 1 clinical trials of a selective Rho kinase inhibitor, K-115, JAMA Ophthalmol. 131 (2013) 1288–1295, https://doi.org/10.1001/jamaophthalmol.2013.323.

[68] R. Roskoski Jr., Vascular endothelial growth factor (VEGF) signaling in tumor progression, Crit. Rev. Oncol. Hematol. 62 (2007) 179–213, https://doi.org/10.1016/j.critrevonc.2007.01.006.
[69] R. Roskoski Jr., VEGF receptor protein-tyrosine kinases: structure and regulation, Biochem Biophys. Res Commun. 375 (2008) 287–291, https://doi.org/10.1016/j.bbrc.2008.07.121.
[70] R. Roskoski Jr., Vascular endothelial growth factor (VEGF) and VEGF receptor inhibitors in the treatment of renal cell carcinomas, Pharmacol. Res 120 (2017) 116–132, https://doi.org/10.1016/j.phrs.2017.03.010.
[71] Z. Tian, X. Niu, W. Yao, Efficacy and response biomarkers of apatinib in the treatment of malignancies in China: a review, Front Oncol. 11 (2021), 749083, https://doi.org/10.3389/fonc.2021.749083.
[72] Y.J. Mi, Y.J. Liang, H.B. Huang, H.Y. Zhao, C.P. Wu, F. Wang, L.Y. Tao, C. Z. Zhang, C.L. Dai, A.K. Tiwari, X.X. Ma, K.K. To, S.V. Ambudkar, Z.S. Chen, L. W. Fu, Apatinib (YN968D1) reverses multidrug resistance by inhibiting the efflux function of multiple ATP-binding cassette transporters, Cancer Res 70 (2010) 7981–7991.
[73] S. Tian, H. Quan, C. Xie, H. Guo, F. Lü, Y. Xu, J. Li, L. Lou, YN968D1 is a novel and selective inhibitor of vascular endothelial growth factor receptor-2 tyrosine kinase with potent activity in vitro and in vivo, Cancer Sci. 102 (2011) 1374–1380, https://doi.org/10.1111/j.1349-7006.2011.01939.x.
[74] X. Hu, J. Zhang, B. Xu, Z. Jiang, J. Ragaz, Z. Tong, Q. Zhang, X. Wang, J. Feng, D. Pang, M. Fan, J. Li, B. Wang, Z. Wang, Q. Zhang, S. Sun, C. Liao, Multicenter phase ii study of apatinib, a novel VEGFR inhibitor in heavily pretreated patients with metastatic triple-negative breast cancer, Int. J. Cancer 135 (2014) 1961–1969.
[75] R. Roskoski Jr., STI-571: an anticancer protein-tyrosine kinase inhibitor, Biochem Biophys. Res Commun. 309 (2003) 709–717, https://doi.org/10.1016/j.bbrc.2003.08.055.
[76] R. Roskoski Jr., Targeting BCR-Abl in the treatment of Philadelphia-chromosome positive chronic myelogenous leukemia, Pharmacol. Res 178 (2022), 106156, https://doi.org/10.1016/j.phrs.2022.106156.
[77] S.H. Kim, H. Menon, S. Jootar, T. Saikia, J.Y. Kwak, S.K. Sohn, J.S. Park, S. H. Jeong, H.J. Kim, Y.K. Kim, S.J. Oh, H. Kim, D.Y. Zang, J.S. Chung, H.J. Shin, Y. R. Do, J.A. Kim, D.Y. Kim, C.W. Choi, S. Park, H.L. Park, G.Y. Lee, D.J. Cho, J. S. Shin, D.W. Kim, Efficacy and safety of radotinib in chronic phase chronic myeloid leukemia patients with resistance or intolerance to BCR-ABL1 tyrosine kinase inhibitors, Haematologica 99 (2014) 1191–1196, https://doi.org/10.3324/haematol.2013.096776.
[78] M.S. Zabriskie, N.A. Vellore, K.C. Gantz, M.W. Deininger, T. O'Hare, Radotinib is an effective inhibitor of native and kinase domain-mutant BCR-ABL1, Leukemia 29 (2015) 1939–1942, https://doi.org/10.1038/leu.2015.42.
[79] A.E. Eskazan, D. Keskin, Radotinib and its clinical potential in chronic-phase chronic myeloid leukemia patients: an update, Ther. Adv. Hematol. 8 (2017) 237–243, https://doi.org/10.1177/2040620717719851.
[80] J.Y. Kwak, S.H. Kim, S.J. Oh, D.Y. Zang, H. Kim, J.A. Kim, Y.R. Do, H.J. Kim, J. S. Park, C.W. Choi, W.S. Lee, Y.C. Mun, J.H. Kong, J.S. Chung, H.J. Shin, D. Y. Kim, J. Park, C.W. Jung, U. Bunworasate, N.S. Comia, S. Jootar, A. H. Reksodiputro, P.B. Caguioa, S.E. Lee, D.W. Kim, Phase III clinical trial (rerise study) results of efficacy and safety of radotinib compared with imatinib in newly diagnosed chronic phase chronic myeloid leukemia, Clin. Cancer Res 23 (2017) 7180–7188.
[81] E.S. Kim, Olmutinib: first global approval, Drugs 76 (2016) 1153–1157.
[82] A. Murtuza, A. Bulbul, J.P. Shen, P. Keshavarzian, B.D. Woodward, F.J. Lopez-Diaz, S.M. Lippman, H. Husain, Novel third-generation EGFR tyrosine kinase inhibitors and strategies to overcome therapeutic resistance in lung cancer, Cancer Res 79 (2019) 689–698, https://doi.org/10.1158/0008-5472.CAN-18-1281.
[83] K. Park, P.A. Jänne, D.W. Kim, J.Y. Han, M.F. Wu, J.S. Lee, J.H. Kang, D.H. Lee, B. C. Cho, C.J. Yu, Y.K. Pang, E. Felip, H. Kim, E. Baek, Y.S. Noh, Olmutinib in T790M-positive non-small cell lung cancer after failure of first-line epidermal growth factor receptor-tyrosine kinase inhibitor therapy: A global, phase 2 study, Cancer 127 (2021) 1407–1416, https://doi.org/10.1002/cncr.33385.
[84] X.S. Hu, X.H. Han, S. Yang, N. Li, L. Wang, Y.Y. Song, H. Mu, Y.K. Shi, Safety, tolerability, and pharmacokinetics of simotinib, a novel specific EGFR tyrosine kinase inhibitor, in patients with advanced non-small cell lung cancer: results of a phase Ib trial, 4449–4449, Cancer Manag Res 11 (2019), https://doi.org/10.2147/CMAR.S189626.
[85] Y.Y. Syed, Anlotinib: first global approval, Drugs 78 (2018) 1057–1062.
[86] C. Xie, X. Wan, H. Quan, M. Zheng, L. Fu, Y. Li, L. Lou, Preclinical characterization of anlotinib, a highly potent and selective vascular endothelial growth factor receptor-2 inhibitor, Cancer Sci. 109 (2018) 1207–1219.
[87] M. Zhou, X. Chen, H. Zhang, L. Xia, X. Tong, L. Zou, R. Hao, J. Pan, X. Zhao, D. Chen, Y. Song, Y. Qi, L. Tang, Z. Liu, R. Gao, Y. Shi, Z. Yang, China National Medical Products Administration approval summary: anlotinib for the treatment of advanced non-small cell lung cancer after two lines of chemotherapy, Cancer Commun. (Lond.) 39 (2019) 36, https://doi.org/10.1186/s40880-019-0383-7.
[88] Y. Gao, P. Liu, R. Shi, Anlotinib as a molecular targeted therapy for tumors, Oncol. Lett. 20 (2020) 1001–1014, https://doi.org/10.3892/ol.2020.11685.
[89] M. Shirley, Fruquintinib: first global approval, Drugs 78 (16) (2018) 1757–1761, https://doi.org/10.1007/s40265-018-0998-z.
[90] D. Lavacchi, G. Roviello, A. Guidolin, S. Romano, J. Venturini, E. Caliman, A. Vannini, E. Giommoni, E. Pellegrini, M. Brugia, S. Pillozzi, L. Antonuzzo, Evaluation of fruquintinib in the continuum of care of patients with colorectal cancer, Int J. Mol. Sci. 24 (2023) 5840, https://doi.org/10.3390/ijms24065840.
[91] X. Yao, N. Du, S. Hu, L. Wang, J. Gao, Rapid advances in research on and development of anticancer drugs in China, Biosci. Trends 13 (2019) 461–464, https://doi.org/10.5582/bst.2019.01243.
[92] J. Zhao, H. Quan, Y. Xu, X. Kong, L. Jin, L. Lou, Flumatinib, a selective inhibitor of BCR-ABL/PDGFR/KIT, effectively overcomes drug resistance of certain KIT mutants, Cancer Sci. 105 (2014) 117–125, https://doi.org/10.1111/cas.12320.
[93] L. Zhang, L. Meng, B. Liu, Y. Zhang, H. Zhu, J. Cui, A. Sun, Y. Hu, J. Jin, H. Jiang, X. Zhang, Y. Li, L. Liu, W. Zhang, X. Liu, J. Gu, J. Qiao, G. Ouyang, X. Liu, J. Luo, M. Jiang, X. Xie, J. Li, C. Zhao, M. Zhang, T. Yang, J. Wang, Flumatinib versus imatinib for newly diagnosed chronic phase chronic myeloid leukemia: a phase iii, randomized, open-label, multi-center FESTnd study, Clin. Cancer Res 27 (2021) 70–77, https://doi.org/10.1158/1078-0432.CCR-20-1600.
[94] S. Dhillon, S.J. Keam, Filgotinib: first approval, Drugs 80 (2020) 1987–1997, https://doi.org/10.1007/s40265-020-01439-0.
[95] R. Roskoski Jr., Janus kinase (JAK) inhibitors in the treatment of inflammatory and neoplastic diseases, Pharmacol. Res 111 (2016) 784–803, https://doi.org/10.1016/j.phrs.2016.07.038.
[96] R. Roskoski Jr., Janus kinase (JAK) inhibitors in the treatment of neoplastic and inflammatory disorders, Pharmacol. Res 183 (2022), 106362, https://doi.org/10.1016/j.phrs.2022.106362.
[97] C.J. Menet, S.R. Fletcher, G. Van Lommen, R. Geney, J. Blanc, K. Smits, N. Jouannigot, P. Deprez, E.M. van der Aar, P. Clement-Lacroix, L. Lepescheux, R. Galien, B. Vayssiere, L. Nelles, T. Christophe, R. Brys, M. Uhring, F. Ciesielski, L. Van Rompaey, Triazolopyridines as selective JAK1 inhibitors: from hit identification to GLPG0634, J. Med Chem. 57 (2014) 9323–9342, https://doi.org/10.1021/jm501262q.
[98] M. Nagasaka, V.W. Zhu, S.M. Lim, M. Greco, F. Wu, S.I. Ou, Beyond Osimertinib: The development of third-generation EGFR tyrosine kinase inhibitors for advanced *EGFR*+ NSCLC, J. Thorac. Oncol. 16 (2021) 740–763, https://doi.org/10.1016/j.jtho.2020.11.028.
[99] L. Chen, Y. Zhou, C. Gan, X. Wang, Y. Liu, C. Dong, R. He, J. Yang, Three third-generation epidermal growth factor receptor tyrosine kinase inhibitors in non-small cell lung cancer: similarities and differences, Cancer Invest 40 (2022) 590–603, https://doi.org/10.1080/07357907.2022.2069254.
[100] S. Dhillon, Tirabrutinib: first approval, Drugs 80 (2020) 835–840.
[101 W. Munakata, K. Tobinai, Tirabrutinib hydrochloride for B-cell lymphomas, Drugs Today 57 (2021) 277–289.
[102] A. Alu, H. Lei, X. Han, Y. Wei, X. Wei, BTK inhibitors in the treatment of hematological malignancies and inflammatory diseases: mechanisms and clinical studies, J. Hematol. Oncol. 15 (2022), 138, https://doi.org/10.1186/s13045-022-01353-w.
[103] R. Roskoski Jr., Ibrutinib inhibition of Bruton protein-tyrosine kinase (BTK) in the treatment of B cell neoplasms, Pharmacol. Res 113 (2016) 395–408, https://doi.org/10.1016/j.phrs.2016.09.011.
[104] R. Roskoski Jr., Blockade of mutant RAS oncogenic signaling with a special emphasis on KRAS, Pharmacol. Res 172 (2021), 105806, https://doi.org/10.1016/j.phrs.2021.105806.
[105] R. Roskoski Jr., Targeting oncogenic Raf protein-serine/threonine kinases in human cancers, Pharmacol. Res 135 (2018) 239–258, https://doi.org/10.1016/j.phrs.2018.08.013.
[106] R. Roskoski Jr., MEK1/2 dual-specificity protein kinases: structure and regulation, Biochem Biophys. Res Commun. 417 (2012) 5–10, https://doi.org/10.1016/j.bbrc.2011.11.145.
[107] R. Roskoski Jr., Allosteric MEK1/2 inhibitors including cobimetanib and trametinib in the treatment of cutaneous melanomas, Pharmacol. Res 117 (2017) 20–31, https://doi.org/10.1016/j.phrs.2016.12.009.
[108] R. Roskoski Jr., ERK1/2 MAP kinases: structure, function, and regulation, Pharmacol. Res 66 (2012) 105–143, https://doi.org/10.1016/j.phrs.2012.04.005.
[109] R. Roskoski Jr., Targeting ERK1/2 protein-serine/threonine kinases in human cancers, Pharmacol. Res 142 (2019) 151–168, https://doi.org/10.1016/j.phrs.2019.01.039.
[110] A.T. Bender, A. Gardberg, A. Pereira, T. Johnson, Y. Wu, R. Grenningloh, J. Head, F. Morandi, P. Haselmayer, L. Liu-Bujalski, Ability of Bruton's tyrosine kinase inhibitors to sequester y551 and prevent phosphorylation determines potency for inhibition of Fc receptor but not B-cell receptor signaling, Mol. Pharm. 91 (2017) 208–219, https://doi.org/10.1124/mol.116.107037.
[111] R. Kozaki, M. Vogler, H.S. Walter, S. Jayne, D. Dinsdale, R. Siebert, M.J.S. Dyer, T. Yoshizawa, Responses to the selective bruton's tyrosine kinase (BTK) inhibitor tirabrutinib (ONO/GS-4059) in diffuse large B-cell lymphoma cell lines, Cancers (Basel) 10 (2018) 127, https://doi.org/10.3390/cancers10040127.
[112] J. Wu, M. Zhang, D. Liu, Bruton tyrosine kinase inhibitor ONO/GS-4059: from bench to bedside, Oncotarget 8 (4) (2017 24) 7201–7207, https://doi.org/10.18632/oncotarget.12786.
[113] S. Dhillon, Delgocitinib: first approval, Drugs 80 (2020) 609–615.
[114] A. Tanimoto, Y. Ogawa, C. Oki, Y. Kimoto, K. Nozawa, W. Amano, S. Noji, M. Shiozaki, A. Matsuo, Y. Shinozaki, M. Matsushita, Pharmacological properties of JTE-052: a novel potent JAK inhibitor that suppresses various inflammatory responses in vitro and in vivo, Inflamm. Res 64 (2015) 41–51, https://doi.org/10.1007/s00011-014-0782-9.
[115] S. Noji, Y. Hara, T. Miura, H. Yamanaka, K. Maeda, A. Hori, H. Yamamoto, S. Obika, M. Inoue, Y. Hase, T. Orita, S. Doi, T. Adachi, A. Tanimoto, C. Oki, Y. Kimoto, Y. Ogawa, T. Negoro, H. Hashimoto, M. Shiozaki, Discovery of a janus kinase inhibitor bearing a highly three-dimensional spiro scaffold: JTE-052 (delgocitinib) as a new dermatological agent to treat inflammatory skin disorders,

J. Med Chem. 63 (2020) 7163–7185, https://doi.org/10.1021/acs.jmedchem.0c00450.
[116] H. Nakagawa, O. Nemoto, A. Igarashi, H. Saeki, H. Kaino, T. Nagata, Delgocitinib ointment, a topical Janus kinase inhibitor, in adult patients with moderate to severe atopic dermatitis: A phase 3, randomized, double-blind, vehicle-controlled study and an open-label, long-term extension study, J. Am. Acad. Dermatol. 82 (2020) 823–831, https://doi.org/10.1016/j.jaad.2019.12.015.
[117] H. Blair, Pyrotinib: first global approval, Drugs 78 (2018) 1751–1755.
[118] B. Xu, M. Yan, F. Ma, X. Hu, J. Feng, Q. Ouyang, Z. Tong, H. Li, Q. Zhang, T. Sun, X. Wang, Y. Yin, Y. Cheng, W. Li, Y. Gu, Q. Chen, J. Liu, J. Cheng, C. Geng, S. Qin, S. Wang, J. Lu, K. Shen, Q. Liu, X. Wang, H. Wang, T. Luo, J. Yang, Y. Wu, Z. Yu, X. Zhu, C. Chen, J. Zou, PHOEBE Investigators, Pyrotinib plus capecitabine versus lapatinib plus capecitabine for the treatment of HER2-positive metastatic breast cancer (PHOEBE): a multicentre, open-label, randomised, controlled, phase 3 trial, Lancet Oncol. 22 (2021) 351–360, https://doi.org/10.1016/S1470-2045(20)30702-6.
[119] Q. Chen, D. Ouyang, M. Anwar, N. Xie, S. Wang, P. Fan, L. Qian, G. Chen, E. Zhou, L. Guo, X. Gu, B. Ding, X. Yang, L. Liu, C. Deng, Z. Xiao, J. Li, Y. Wang, S. Zeng, J. Hu, W. Zhou, B. Qiu, Z. Wang, J. Weng, M. Liu, Y. Li, T. Tang, J. Wang, H. Zhang, B. Dai, W. Tang, T. Wu, M. Xiao, X. Li, H. Liu, L. Li, W. Yi, Q. Ouyang, Effectiveness and safety of pyrotinib, and association of biomarker with progression-free survival in patients with her2-positive metastatic breast cancer: a real-world, multicentre analysis, Front Oncol. 10 (2020), 811, https://doi.org/10.3389/fonc.2020.00811.
[120] W. Hu, J. Yang, Z. Zhang, D. Xu, N. Li, Pyrotinib for HER2-positive metastatic breast cancer: a systematic review and meta-analysis, Transl. Cancer Res 12 (2023) 247–256, https://doi.org/10.21037/tcr-22-1746.
[121] M. Zhang, Z. Yu, X. Yao, Z. Lei, K. Zhao, W. Wang, X. Zhang, X. Chen, D. Liu, Prediction of pyrotinib exposure based on physiologically-based pharmacokinetic model and endogenous biomarker, Front Pharm. 13 (2022), 972411, https://doi.org/10.3389/fphar.2022.972411.
[122] S. Dhillon, Orelabrutinib: first approval, Drugs 81 (2021) 503–507.
[123] W. Xu, K. Zhou, T. Wang, S. Yang, L. Liu, Y. Hu, W. Zhang, K. Ding, J. Zhou, S. Gao, B. Xu, Z. Zhu, T. Liu, H. Zhang, J. Hu, C. Ji, S. Wang, Z. Xia, X. Wang, Y. Li, Y. Song, S. Ma, X. Tang, B. Zhang, J. Li, Orelabrutinib in relapsed or refractory chronic lymphocytic leukemia/small lymphocytic lymphoma patients: Multi-center, single-arm, open-label, phase 2 study, Am. J. Hematol. 98 (2023) 571–579, https://doi.org/10.1002/ajh.26826. Has IC50 1.6nM.
[124] A. Markham, S.J. Keam, Peficitinib: first global approval, Drugs 79 (2019) 887–891.
[125] H. Hamaguchi, Y. Amano, A. Moritomo, S. Shirakami, Y. Nakajima, K. Nakai, N. Nomura, M. Ito, Y. Higashi, T. Inoue, Discovery and structural characterization of peficitinib (ASP015K) as a novel and potent JAK inhibitor, Bioorg. Med Chem. 26 (2018) 4971–4983, https://doi.org/10.1016/j.bmc.2018.08.005.
[126] S. Kubo, S. Nakayamada, Y. Tanaka, JAK inhibitors for rheumatoid arthritis, Expert Opin. Invest. Drugs 32 (2023) 333–344, https://doi.org/10.1080/13543784.2023.2199919.
[127] Y.Y. Syed, Surufatinib: first approval, Drugs 81 (2021) 727–732, https://doi.org/10.1007/s40265-021-01489-y.
[128] J. Xu, Current treatments and future potential of surufatinib in neuroendocrine tumors (NETs), 17588359211042689, Ther. Adv. Med Oncol. 13 (2021), https://doi.org/10.1177/17588359211042689.
[129] R. Roskoski Jr., The role of fibroblast growth factor receptor (FGFR) protein-tyrosine kinase inhibitors in the treatment of cancers including those of the urinary bladder, Pharmacol. Res 151 (2020), 104567, https://doi.org/10.1016/j.phrs.2019.104567.
[130] C. Xiang, H. Li, W. Tang, Targeting CSF-1R represents an effective strategy in modulating inflammatory diseases, Pharmacol. Res 187 (2023), 106566, https://doi.org/10.1016/j.phrs.2022.106566.
[131] T. Cai, Y. Cheng, Y. Du, P. Tan, T. Li, Y. Chen, L. Gao, W. Fu, Efficacy and safety of surufatinib in the treatment of advanced solid tumors: a systematic evaluation and meta-analysis, Oncol. Lett. 25 (2023), 273, https://doi.org/10.3892/ol.2023.13859.
[132] M.A. Ali, S.S. Shah, N. Tahir, S. Rehman, M. Saeed, S.F. Bajwa, R. Ali, W. Aiman, M.Y. Anwar, Efficacy and toxicity of surufatinib in neuroendocrine tumors: A systematic review and meta-analysis, J. Neuroendocr. 34 (2022), e13149, https://doi.org/10.1111/jne.13149.
[133] A. Markham, Savolitinib: first approval, Drugs 81 (2021) 1665–1670, https://doi.org/10.1007/s40265-021-01584-0.
[134] M. Sakamoto, T. Patil, MET alterations in advanced non-small cell lung cancer, Lung Cancer 178 (2023) 254–268, https://doi.org/10.1016/j.lungcan.2023.02.018.
[135] M.M. Frigault, A. Markovets, B. Nuttall, K.M. Kim, S.H. Park, E.A. Gangolli, P.G. S. Mortimer, S.J. Hollingsworth, J.Y. Hong, K. Kim, S.T. Kim, J.C. Barrett, J. Lee, Mechanisms of acquired resistance to savolitinib, a selective MET inhibitor in *MET*-amplified gastric cancer, JCO Precis Oncol. (4) (2020), PO.19.00386, https://doi.org/10.1200/PO.19.00386.
[136] M. Zaborowska-Szmi, S. Szmit, M. Krzakowski, D.M. Kowalski, Savolitinib for non-small cell lung cancer, Drugs Today 59 (2023) 17–36, https://doi.org/10.1358/dot.2023.59.1.3425324.
[137] X. Zhu, Y. Lu, S. Lu, Landscape of savolitinib development for the treatment of non-small cell lung cancer with MET alteration-a narrative review, Cancers (Basel) 14 (2022) 6122, https://doi.org/10.3390/cancers14246122.
[138] S. Dhillon, Lazertinib: first approval, Drugs 81 (9) (2021) 1107–1113, https://doi.org/10.1007/s40265-021-01533-x.
[139] J. Yun, M.H. Hong, S.Y. Kim, C.W. Park, S. Kim, M.R. Yun, H.N. Kang, K.H. Pyo, S. S. Lee, J.S. Koh, H.J. Song, D.K. Kim, Y.S. Lee, S.W. Oh, S. Choi, H.R. Kim, B. C. Cho, YH25448, an irreversible EGFR-TKI with potent intracranial activity in EGFR mutant non-small cell lung cancer, Clin. Cancer Res 25 (2019) 2575–2587, https://doi.org/10.1158/1078-0432.CCR-18-2906.
[140] E.D. Deeks, Furmonertinib: first approval, Drugs 81 (2021) 1775–1780, https://doi.org/10.1007/s40265-021-01588-w.
[141] S.C.M. Lau, S.I. Ou, And still they come over troubled waters: Can Asia's third-generation EGFR tyrosine kinase inhibitors (furmonertinib, aumolertinib, rezivertinib, limertinib, befotertinib, sh-1028, and lazertinib) affect global treatment of EGFR+ NSCLC, J. Thorac. Oncol. 17 (2022) 1144–1154, https://doi.org/10.1016/j.jtho.2022.08.016.
[142] C.A. Lipinski, F. Lombardo, B.W. Dominy, P.J. Feeney, Experimental and computational approaches to estimate solubility and permeability in drug discovery and development settings, Adv. Drug Deliv. Rev. 46 (2001) 3–26, https://doi.org/10.1016/s0169-409x(00)00129-0.
[143] R. Roskoski Jr., Rule of five violations among the FDA-approved small molecule protein kinase inhibitors, Pharmacol. Res 191 (2023), 106774, https://doi.org/10.1016/j.phrs.2023.106774.
[144] A.L. Hopkins, C.R. Groom, A. Alex, Ligand efficiency: a useful metric for lead selection, Drug Discov. Today 9 (2004) 430–431, https://doi.org/10.1016/S1359-6446(04)03069-7.
[145] P.D. Leeson, B. Springthorpe, The influence of drug-like concepts on decision-making in medicinal chemistry, Nat. Rev. Drug Discov. 6 (2007) 881–890, https://doi.org/10.1038/nrd2445.
[146] S. Ekins, N.K. Litterman, C.A. Lipinski, B.A. Bunin, Thermodynamic proxies to compensate for biases in drug discovery methods, Pharm. Res 33 (2016) 194–205, https://doi.org/10.1007/s11095-015-1779-y.
[147] A.L. Hopkins, G.M. Keserü, P.D. Leeson, D.C. Rees, C.H. Reynolds, The role of ligand efficiency metrics in drug discovery, Nat. Rev. Drug Discov. 13 (2014) 105–121, https://doi.org/10.1038/nrd4163.
[148] P.D. Leeson, Molecular inflation, attrition, and the rule of five. Adv. Drug Deliv. Rev. 101 (2016) 22–33, https://doi.org/10.1016/j.addr.2016.01.018.
[149] D.F. Veber, S.R. Johnson, H.Y. Cheng, B.R. Smith, K.W. Ward, K.D. Kopple, Molecular properties that influence the oral bioavailability of drug candidates, J. Med Chem. 45 (2002) 2615–2623, https://doi.org/10.1021/jm020017n.
[150] T.I. Oprea, Property distribution of drug-related chemical databases, J. Comput. Aided Mol. Des. 14 (2000) 251–264, https://doi.org/10.1023/a:1008130001697.
[151] P.D. Leeson, A.P. Bento, A. Gaulton, A. Hersey, E.J. Manners, C.J. Radoux, A. R. Leach, Target-based evaluation of "drug-like" properties and ligand efficiencies, J. Med Chem. 64 (2021) 7210–7230, https://doi.org/10.1021/acs.jmedchem.1c00416.
[152] T.W. Johnson, R.A. Gallego, M.P. Edwards, Lipophilic efficiency as an important metric in drug design, J. Med Chem. 61 (2018) 6401–6420, https://doi.org/10.1021/acs.jmedchem.8b00077.
[153] T.J. Ritchie, S.J. Macdonald, Physicochemical descriptors of aromatic character and their use in drug discovery, J. Med Chem. 57 (2014) 7206–7215, https://doi.org/10.1021/jm500515d.
[154] S.H. Bertz, The first general index of molecular complexity, J. Am. Chem. Soc. 1103 (1981) 3559–3601.
[155] J.B. Hendrickson, P. Huang, A.G. Toczko, Molecular complexity: a simplified formula adapted to individual atoms, J. Chem. Inf. Compout Sci. 27 (1987) 63–67.
[156] F. Lovering, J. Bikker, C. Humblet, Escape from flatland: increasing saturation as an approach to improving clinical success, J. Med Chem. 52 (2009) 6752–6756, https://doi.org/10.1021/jm901241e.
[157] B.C. Doak, J. Zheng, D. Dobritzsch, J. Kihlberg, How beyond rule of 5 drugs and clinical candidates bind to their targets, J. Med Chem. 59 (2016) 2312–2327, https://doi.org/10.1021/acs.jmedchem.5b01286.
[158] L. Huang, S. Jiang, Y. Shi, Tyrosine kinase inhibitors for solid tumors in the past 20 years (2001-2020), J. Hematol. Oncol. 13 (2020), 143, https://doi.org/10.1186/s13045-020-00977-0.
[159] K. Bechman, M. Yates, J.B. Galloway, The new entries in the therapeutic armamentarium: The small molecule JAK inhibitors, Pharmacol. Res 147 (2019), 104392, https://doi.org/10.1016/j.phrs.2019.104392. Corrigendum doi: 10.1016/j.phrs.2020.104634.
[160] Bechman K., Galloway G.B., Winthrop K.L. Small-molecule protein kinase inhibitors and the risk of fungal infections. Curr Fungal Infect Rep. 10.1007/s12281–019-00350-w.
[161] C.I. Wells, H. Al-Ali, D.M. Andrews, C.R.M. Asquith, A.D. Axtman, I. Dikic, D. Ebner, P. Ettmayer, C. Fischer, M. Frederiksen, R.E. Futrell, N.S. Gray, S. B. Hatch, S. Knapp, U. Lücking, M. Michaelides, C.E. Mills, S. Müller, D. Owen, A. Picado, K.S. Saikatendu, M. Schröder, A. Stolz, M. Tellechea, B.J. Turunen, S. Vilar, J. Wang, W.J. Zuercher, T.M. Willson, D.H. Drewry, The kinase chemogenomic set (KCGS): an open science resource for kinase vulnerability identification, Int J. Mol. Sci. 22 (2021) 566, https://doi.org/10.3390/ijms22020566.
[162] J. Choo, G. Heo, C. Pothoulakis, E. Im, Posttranslational modifications as therapeutic targets for intestinal disorders, Pharmacol. Res (2021), 105412, https://doi.org/10.1016/j.phrs.2020.105412.
[163] Z. Xie, X. Yang, Y. Duan, J. Han, C. Liao, Small-molecule kinase inhibitors for the treatment of nononcologic diseases, J. Med Chem. 64 (2021) 1283–1345.
[164] A. Cichońska, B. Ravikumar, R.J. Allaway, F. Wan, S. Park, O. Isayev, S. Li, M. Mason, A. Lamb, Z. Tanoli, M. Jeon, S. Kim, M. Popova, S. Capuzzi, J. Zeng, K. Dang, G. Koytiger, J. Kang, C.I. Wells, T.M. Willson, , IDG-DREAM Drug-Kinase Binding Prediction Challenge Consortium, Oprea TI, A. Schlessinger, D.

H. Drewry, G. Stolovitzky, K. Wennerberg, J. Guinney, T. Aittokallio, Crowdsourced mapping of unexplored target space of kinase inhibitors, Nat. Commun. 12 (2021), 3307, https://doi.org/10.1038/s41467-021-23165-1.
[165] X. Lu, J.B. Smaill, K. Ding, New promise and opportunities for allosteric kinase inhibitors, Angew. Chem. Int Ed. Engl. 59 (2020) 13764–13776, https://doi.org/10.1002/anie.201914525.
[166] M. Zhang, Y. Liu, H. Jang, R. Nussinov, Strategy toward kinase-selective drug discovery, J. Chem. Theory Comput. 19 (2023) 1615–1628, https://doi.org/10.1021/acs.jctc.2c01171.
[167] R. Macarron, M.N. Banks, D. Bojanic, D.J. Burns, D.A. Cirovic, T. Garyantes, D. V. Green, R.P. Hertzberg, W.P. Janzen, J.W. Paslay, U. Schopfer, G. S. Sittampalam, Impact of high-throughput screening in biomedical research, Nat. Rev. Drug Discov. 10 (2011) 188–195, https://doi.org/10.1038/nrd3368.
[168] I.V. Hartung, B.R. Huck, A. Crespo, Rules were made to be broken, Nat. Rev. Chem. (2023), https://doi.org/10.1038/s41570-022-00451-0.
[169] R. Roskoski Jr., Guidelines for preparing color figures for everyone including the colorblind, Pharmacol. Res 119 (2017) 240–241, https://doi.org/10.1016/j.phrs.2017.02.005. Erratum in: Pharmacol Res 2019;139:569. doi: 10.1016/j.phrs.2018.09.019.